Università degli Studi di Palermo

Dottorato di Ricerca in

Medicina Sperimentale e Molecolare

Coordinatore: Prof. Giovanni Zummo

Sede Amministrativa:
Dipartimento di Biomedicina Sperimentale e Neuroscienze Cliniche

Role of microRNAs in fetal heart development and in isolated cardiac progenitor cells

Dott.ssa Claudia Serradifalco

Relatore: Chiar.mo Prof G. Zummo

Co-relatore: Chiar.ma Dott.ssa V. Di Felice

(SSD BIO/16) Anatomia Umana

XXIII CICLO

1. INTRODUCTION

1.1 Heart development

The heart is one of the first embryonic organs to start functioning. It originates from the splanchnic mesoderm. One of the first event that occurs during heart development is the specification and migration of cardiac precursor cells. At the earliest stages of heart formation, two pools of cardiac precursors are present: the First Heart Field (FHF), which contributes to the left ventricle, and the second heart field (SHF), which gives rise to a large portion of the heart, including the right ventricle first and to the outflow tract, sinus venosus and left and right atria later. SHF is subdivided into several lineage pools which contribute either to anterior structures or posterior components. These findings explain why mutations associated with congenital cardiac diseases result in defects of specific heart structures. The following step in heart formation is the movement of cardiac precursors which aggregate forming the “heart tube” [1]. In human development, during this phase the heart starts beating. After the formation of the heart tube, two epithelial layers, separated by an acellular matrix, called “cardiac jelly”, are observed. These two layers are the myocardium and the endocardium [2]. Hence the heart tube is made up of three layers: the outer one, called epicardium, the middle one, myocardium, and the inner layer, endocardium.

During the course of development, the heart loops towards the right side and subsequently the atrial and ventricular segments become recognizable. The following phase is characterized by the formation of septa which give rise to two atria, two ventricles, two atrioventricular canals (which will become valves) and the outflow tract (Figure 1A). Later, endocardial cells move into the cardiac jelly forming the “cardiac cushion” which will give rise to the atrioventricular valves, and the ventricular septation arises from myocardium from the left and right ventricles. Following the formation of the “primary atrium septum” and the “secondary atrium septum” the separation of atria into right and left portions occurs. The latest event concerning septation of the heart occurs in the outflow tract region where the common outflow is divided into the aorta, connected to the left ventricle, and pulmonary artery, connected to the right ventricle (Figure. 1B) [3]. At the end of the septation process, part of the outflow tract disappears and

part becomes incorporated into the ventricular chambers. Thus, the flanking segments are no longer identifiable in the fetal heart.

The mechanisms involved in heart development are finely regulated by a complex network of genes which are differentially expressed in the cardiac compartments. These genes code for cardiac-specific transcription factors, contractile proteins, proteins involved in calcium handling and impulse conduction, for cell-cell and cell-matrix contact molecules. In the last years, a new class of molecules, called microRNAs, have been demonstrated to play a fundamental role during cardiac development.

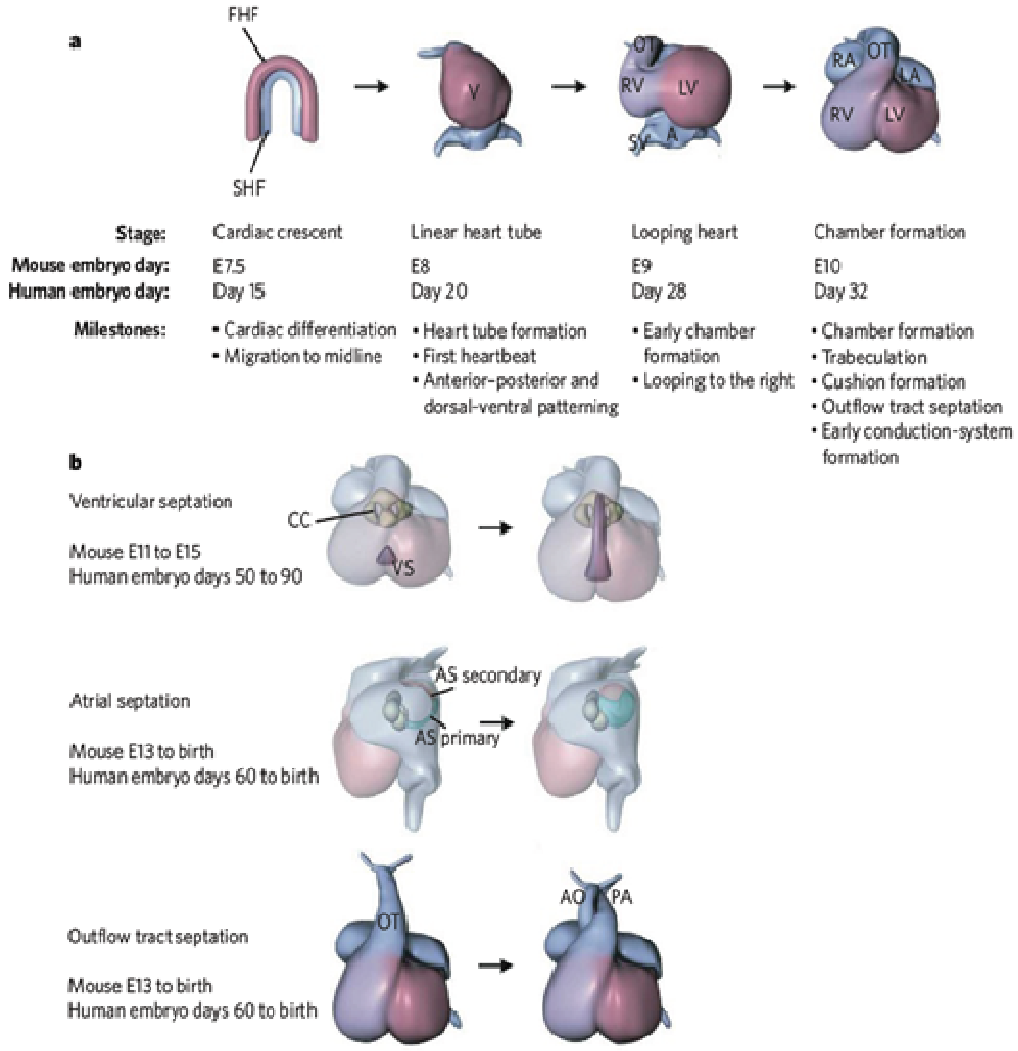

Figure 1. Heart development. Early steps in heart development (A). Maturation of the heart (B) [3].

1.2 MicroRNA

1.2.1 MicroRNA: from yesterday to nowadays

MicroRNAs (miRNAs) are short endogenous single-strand RNA molecules (21-23 nucleotides in length) that inhibit mRNA target translation.

MiRNAs were described, for the first time, in 1993 in *Caenorhabditis elegans* by Lee and colleagues. The authors found a small non-coding RNA, called *Lin-4*, which was able to inhibit the translation of Lin-14 mRNA during the larval development [4]. However, this evaluation came from many studies performed in *Caenorhabditis elegans* starting from 1981, when Chalfie and colleagues found a loss of function mutation in the gene of *lin-4* which led to a constitutive expression of larval-specific genes [5]. Eight years later, another group of researchers demonstrated that *lin-4* was able to inhibit the expression of two genes, lin-14 and lin-28, involved into the larva-to-adult developmental switch [6]. Later, in 1991, through deletion experiments, it was found that the interaction between *lin-4* and lin-14 was required to down-regulate lin-14 protein levels during development [7]. Finally, thanks to these discoveries, in 1993, Lee and colleagues described *lin-4* as a small-non coding RNA which was a negative regulator of lin-14 mRNA; the authors also found that *Lin-4* RNA sequences were complementary to the 3'untranslated region of the Lin-14 messenger, suggesting a potential specific-sequence interaction [4]. Some years later, the discovery of another non-coding small RNA, allowed the development of the research field on miRNAs. In a study performed in 2000 by Reinhart and colleagues, a small RNA (21-nucleotides in length), *let-7*, was described as a regulatory RNA highly conserved among the species [8]. This finding opened the way to other studies that finally recognized the class of small non-coding RNA as a novel class of regulators for gene expression, called microRNAs [9].

At present, for the microRNA study, scientists use a database, called, miRBase (http://www.mirbase.org/) that is actually the primary online repository for all microRNA sequences and annotation. To date, the current release (miRBase 17) contains over 16000 microRNA gene loci in over 150 species, and over 19000 distinct mature microRNA sequences. That means that the miRNA field is rapidly

growing, considering that over 2000 miRNA sequences have been already described in vertebrates, flies, worms and plants, and even in viruses.

1.2.2 Biogenesis

MiR genes are localized either in independent units, with their own promoter, or in introns ("intronic miRNAs") of protein coding genes [10].

MiR are first transcribed as long primary miRNA transcripts ("pri-miRs") by RNA polymerase II inside the nucleus; pri-miR contains a stem-loop structure, a cap at 5'-end and a poly-A tail at 3'-end [11]. Then, pri-miR is cleaved by the enzymatic complex called "microprocessor" in molecules of 70-100 nt in length that take name of "pre-miR" [12]. The microprocessor complex is composed by the ribonuclease III Drosha and its cofactor Di George syndrome critical region gene 8 (DGCR8), a double-strand RNA binding protein required for binding the RNA ds substrate and for facilitating cleavage by Drosha positioning its catalytic sites in the proper manner [13].

Cleavage releases a pre-miR hairpin that is typically ≈ 55–70 nt in length. The 2 nt 3'overhangs of pre-miR hairpin are recognized by Exportin-5 (Exp-5), which is a member of the nuclear transport receptor family, and its partner Ran-GTP, that allows the passage into cytoplasm (Exp-5 binds cooperatively its cargo and its cofactor Ran-GTP: the hydrolysis of GTP allows the cargo release in the cytoplasm) [14]. Here, a second cleavage is generated by the enzyme Dicer, another member of the ribonuclease III family highly conserved among species, which gives rise to 22 nt small RNA duplexes. Dicer associates with ds-RNA-binding proteins, like transactivation-response element RNA-binding protein (TRBP) and p53-associated cellular protein (PACT), which contain dsRNA-binding domains for pre-miR processing [15], [16]. RNA duplex is unwound by helicase activity of Dicer and one of the strands is preferentially incorporated into Argonaute (Ago) protein so as to generate the effector complex RNA induced silencing complex (RISC) [17]. Ago proteins are identified by three characteristic domains: N-terminal PAZ domain, the middle MID domain and the C-terminal PIWI domain [18]. Ago family is very large and it includes several members like

Ago1, Ago2, Ago3. Ago2 seems to be able, alone, to form a cleavage-competent RISC [19].

Strand selection of miRNA may be determined by the relative thermodynamic stability of the two ends of miRNA duplexes [20]: the strand with less stability at the 5'-end (typically a GU pair instead of GC pair) is loaded onto RISC, whereas the other strand, the passenger (miR*), is released [21].

At first it was thought that miR* was degraded soon after its release. However, many evidences demonstrate that miRs* are often present at physiologically levels [22], and that they have many biological roles, for example miR-378* has been identified as a molecular switch in breast cancer cells [23], and miR-155* (together with miR-155) is involved in regulating human plasmacytoid dendritic cell (PDC) activation [24]. Furthermore, substantial fraction of miR* species are stringently conserved over vertebrate evolution, they exhibit greatest conservation in their seed regions, and define complementary motifs whose conservation across vertebrate 3′-UTR evolution is statistically significant [25].

Moreover, it was found that a significant fraction of pre-miR hairpins produces miR* species whose seed sequence recognizes 3'UTR target site. That means that miR* are not present just in cells, but they also acquired endogenous regulatory target [22].

However, according to the official nomenclature, miR* indicates the miR strand which is weakly expressed. If it is not known which of the two strands is more expressed than the other, usually it can be found the indication "miR-5p" and "miR-3p" depending on the position on the genome (5' or 3'-arm of the hairpin).

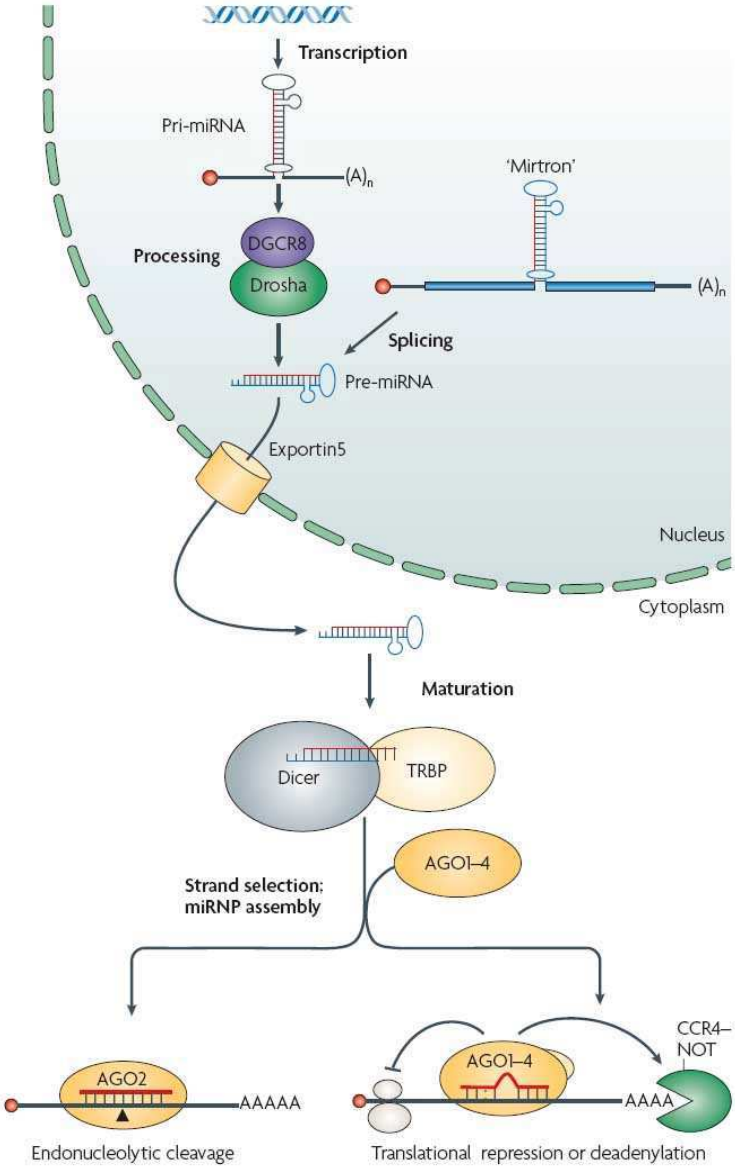

Figure 2. MicroRNA biogenesis and their assembly into ribonucleoproteins [26]

1.2.3 How do microRNAs work?

MicroRNAs have been proposed as “micromanagers” of gene expression, because they might act as on-off switches to eliminate mRNAs that should not be expressed in a specific cell type or at a specific moment. They also can regulate mRNAs abundance, adjusting levels within physiological range [27].

MicroRNAs interact with their mRNA targets by base pairing. In plants, most microRNAs base pair to mRNAs with perfect complementarity, inducing mRNA degradation by a cleavage in the middle of the miRNA-mRNA duplex [28].

In the case of metazoans, generally, the interaction between miRNA and its target is imperfect [29]. The region responsible of this interaction is called “seed sequence” and it corresponds to the nucleotide 2 to 8 (nucleotide 1 is the first one from 5’-end) (Figure 3). Just for thermodynamic reasons, an A nucleotide across position 1, and an A or U across position 9, improve the site efficiency, even if they don’t need to base pair with miRNA nucleotides [30]. Furthermore, there must be a complementarity to the miRNA 3’ half to stabilize the interaction, even if mismatches and bulges (structural motifs formed following a mismatch in the miRNA : mRNA hetroduplex) are tolerated in this region, but, if the interaction with seed region is not perfect, there should be a good base pair to residues 13-16 of the miRNA to give a good stability [31], [29].

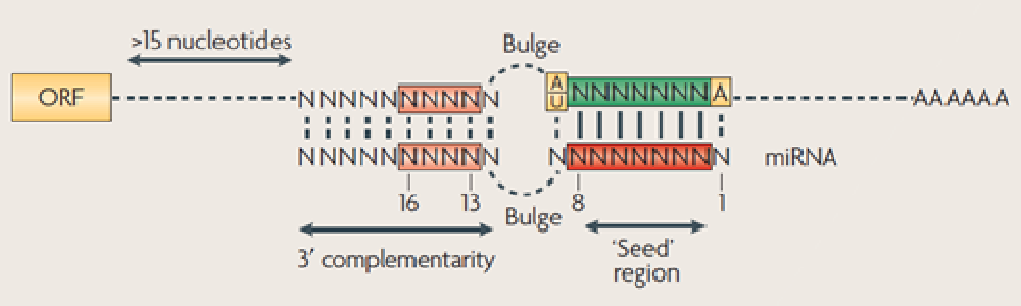

Figure 3. **microRNA-mRNA interaction** [26]

Furthermore, there are many factors that influence the site efficiency, among which an AU-rich neighborhood and, in case of long 3'-UTRs, a position not so far away from the poly-A tail or the termination codon, so that to make binding sites more accessible [29], [32]. In contrast with these rules, there are many cases in which a bulged nucleotide in the seed region is required for an efficient repression miRNA-mediated [26].

Typically, more than one miRNA binding site is present on 3'UTR of mRNA target and multiple sites for the same or different miRNAs are required for effective repression [32], [31], [30], [29]. When they are localized close to each other they act cooperatively providing a stronger repression [30], [29].

MiRNAs act either inhibiting mRNA translation or inducing degradation of target. When the association miRNA-mRNA target presents several mismatches and bulges, it results in a reduced efficiency of translation rather than in a decrease in mRNA abundance [33]. The inhibition of mRNAs translation can occur at the initiation or post-initiation step. In repression at the initiation step, Ago2 protein is the main actor: it has a MC domain (cap-binding like domain) which bind the m^7G cap of mRNA precluding the recruitment of eIF4E and, therefore, the assembly of translation complex [34].

For the repression at post-initiation step a drop-off model is proposed: miRNAs render ribosome prone to premature termination of translation [35]. When miRNAs bind with a strong complementarity to their target, the mRNA degradation is induced by deadenylation in 3' → 5' direction catalyzed by the exosome, or by the removal of the cap followed by 5' → 3' degradation catalyzed by the exoribonuclease-1 (XRN1) [26].

Degradation or, at least, its final steps, seems to occur in P-bodies, that are granules localized in the cytoplasm enriched in mRNA-catabolyzing enzymes and translational repressors [36], [37] (Figure 4). P-bodies are also enriched in Ago proteins and miRNAs. Originally they were considered as being primarily involved in mRNA degradation, but now it is clear that P-bodies are also temporary sites of storage of repressed mRNAs [26].

In particular situations, like following a stress, the mRNA sequestration in P-bodies can be irreversible and it can be released and translated after the interaction with polysomes [38].

Studies that look at a better understanding of miRNAs function always go on and many models are continuously proposed.

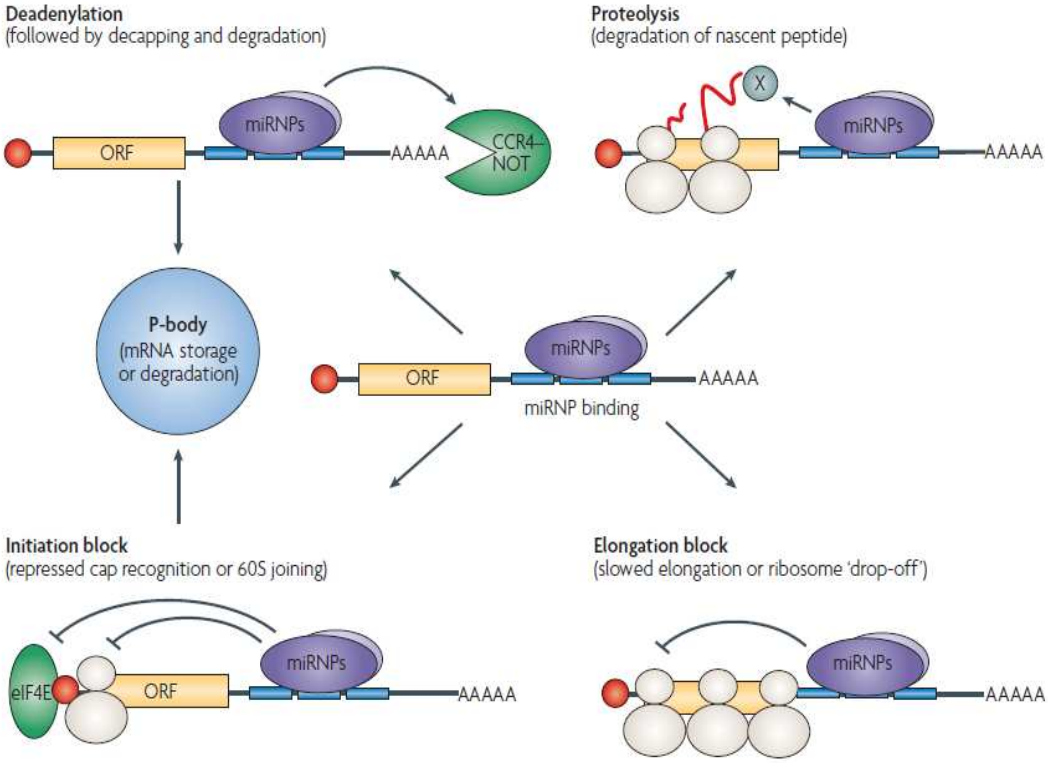

Figure 4. Possible mechanisms of the microRNAs mediated post-transcriptional gene repression in animal cells [26]

1.2.4 MiRNA prediction target

To appreciate the significance of a change in miRNA levels during a particular cellular process, the identification of their own mRNA targets is crucial. To achieve this purpose many computational prediction target tools, based on specific algorithms, have been developed. The most widely utilized engines are miRanda (www.microrna.org), TargetScan (www.targetscan.org) and PicTar (www.pictar.mdc-berlin.de). They are based on algorithms which rely on base-paring between "seed sequence" of the miRNA and the 3'-UTR sequence of the mRNA target but miRNA target sites are localized also within the coding region of a gene even if at much lower frequency. Each engine uses different algorithms to establish the alignment score.

MiRanda calculates the alignment score as the sum of match and mismatch scores, including G:U wobbles and gap penalties. Since sequence conservation is a strong indication of functional constraints in evolution, miRanda prediction software also considers the degree of evolutionary conservation of the targeted sequence and its position in 3'-UTRs of human, mouse and rat genes [39].

TargetScan prediction software applies an alignment score for Watson-Crick base-pairing in the seed sequence (nucleotides 2-7) of the miRNA to its target and also base-pairing beyond the seed sequence that can compensate for mismatches in the seed. It also recognizes a conserved adenosine at the first position and/or a W-C match at position 8, and considers the degree of conservation using three different levels: highly conserved between human, rat, mouse, dog, and chicken; conserved between human, mouse, rat, and dog; poorly conserved among any combination of species [29], [40].

The third target prediction software is PicTar that takes into account a perfect W-C base paired 7 nucleotides seed (1-7 or 2-8) allowing mismatches if the free binding energy does not increase, the binding energy of the entire miRNA-mRNA duplex, and the degree of conservation of targeted sites between all the species (chimpanzee, pufferfish and zebrafish) [41].

Another important criterion that should be considered during miRNA target prediction is the accessibility of the target site. In fact when the target site is

localized in a closed stem structure, the inhibition by miRNA is not allowed. For this reason a prediction software, called Probability of Interaction by Target Accessibility (PITA) was designed; which allows prediction of target sites by first searching for complementary seed sequences, and then calculating the free binding-energy after substracting the energy used to unwind any predicted secondary structure [42].

1.2.5 miRNAs in the heart: implications in cardiac development and diseases

MiRNAs are involved in several physiological and pathological processes as development, apoptosis, cell differentiation, metabolism and cancer and they are often tissue-specific; for example miR-122 is liver-specific, miR-142 and miR-223 are expressed in the hematopoietic system, miR-9, miR-124 and miR-128 are predominant in the nervous system [43].

Many studies have been conducted to shine a light on the importance of microRNAs in the heart. For example, it has been demonstrated that in zebrafish miR-138 is fundamental for the correct development of ventricles and for cardiomyocytes maturation. The loss of miR-138 leads to the expression in ventricular region of the genes whose expression is normally restricted to the atrio-ventricular valve region, and it induces a block of the ventricular cardiomyocyte differentiation [44].

Other studies have established that albeit miR-208, miR-145/miR-143 are abundant in the heart and they play an important role in the cardiomyocytes biology, the disruption of their function do not induce a pathological phenotype during cardiac development in mice.

The importance of miRNAs during cardiac development is confirmed by recent evidences.

In a mouse model, the inactivation of Dicer in cardiac precursor cells was lethal during embryogenesis at E12.5 [45], and mice KO for DGCR8 developed a dilated cardiomyopathy, died of heart deficiency in less than 31 days, and expression levels of miR-1, miR-133 and miR-208, that are cardiac specific, noticeably decreased [46].

Moreover, a study performed in 2007 by Ikeda and colleagues showed the expression of which microRNAs was altered in cardiac diseases; for example in dilated cardiomyopathy (DCM), in ischemic cardiomyopathy (ICM), and in aortic stenosis (AS), the expression levels of miR-1 are decreased whereas miR-214 levels are strongly increased. Furthermore, changes in miRNA levels are not overlapping; this suggests that there is a distinct expression pattern of miRNA in each cardiac disease [47].

1.3 Cardiac Progenitor cells

In the past years the general belief about heart has been that heart was a terminally differentiated postmitotic organ where the number of cardiomyocytes was established at birth and persisted during the life span of the organ. Moreover, the typical cardiac weight gain that occurs during hypertrophy was considered dependent from a rearrange of cytoplasmic organization of cardiomyocytes that grown in volume. However, in the last few years this general belief has been disavowed, in fact several evidences suggest that heart is in continuous turnover and has intrinsic regenerative potential. Mitotic cells have been found in normal and pathological hearts [48] and, afterwards, cardiac precursor or stem cells inside stem niches of the adult myocardium have been identified [49], [50]. A cardiac stem cell (CSC) has specific features: it is self-renewing (able to maintain the undifferentiated state even after many cell cycles), clonogenic (able to expand in culture after plating 1 cell per well), and multipotent that is the ability of differentiating into the three main cardiac lineages: myocytes, smooth muscle cells (SMC), and endothelial cells (EC). On the other hand, a progenitor cell is an immature committed proliferating cell able to differentiate into only one of the three above-mentioned lineages (myocyte or SMC or EC). Actually, there are still no markers that can distinguish a stem from a progenitor cell [51].

The discovery of c-Kit-positive cardiac stem cells, that live in the heart and can differentiate into cardiac cell lineage, has definitely changed the knowledge about myocardial biology. However, the acceptance of the shift in ancient paradigm has been problematic and subjected to criticism. In fact, myocyte death is a normal

event that occurs during human heart diseases; in order to maintain heart vitality, myocyte death has to be accompanied by myocyte regeneration: this is the principle of homeostasis [52]. Moreover, the identification of CSCs has generated several doubts about their role in spontaneous cardiac regeneration after damage. As it is known, the physiological consequences of myocardium infarction are scar tissue formation and loss of mass and contractile function. The fact that resident human CSCs have limitations in reconstructing cardiomyocytes after infarction (this event is considered as the proof that heart is a post-mitotic organ terminally differentiated) [53] could be explained thinking that CSCs, which are present throughout the infarcted myocardium, die by apoptosis and necrosis as the other cells during heart failure [54].

1.3.1 Cardiac Stem Cell classes

After the discovery of c-Kit-positive CSCs, different classes of progenitor cells have been described as ISL1-positive cells, side population progenitors, Sca-1-positive cells and epicardial progenitors. All of them have been considered as distinct CSC classes (Figure 5). However, the unusual number of CSC categories clashes with the features of all self-renewing organ in which a single tissue-specific adult stem cell has been found [54].

1.3.1.1 C-Kit-positive cells

C-Kit-positive CSCs have been described, in rodent, for the first time 9 years ago, by Beltrami and colleagues, as cells with typical features of stem cells (clonogenic, able to divide symmetrically and asymmetrically *in vitro* and differentiate into myocyte, SMC or EC) [55]. *In vivo*, c-Kit^{+} -CSCs seem to be able to partly regenerate the infarcted myocardium differentiating in cardiomyocytes with mechanical and electric properties of functionally competent cells and ameliorating the performance of damaged heart [54].
C-Kit-positive primitive cells have been found also within spherical aggregates, called cardiospheres, formed afterwards cardiac surgical biopsy specimens

culture; these cells have been demonstrated to be positive also to CD105 that is regulatory component of the transforming growth factor-β receptor complex important in angiogenesis and hematopoiesis. Cardiospheres contain also differentiating cells, which express myocytes protein and connexin-43, and an outer layer of mesenchymal stromal cells [56].

The localization of c-Kit positive cells have been also investigated in human adult heart in normal and pathological conditions. A study performed in 2008 showed that the number of c-Kit positive cells is increased in pathological hearts and they are more numerous in the subepicardium rather than in the myocardium; the authors also found that the subepicardium is strongly positive to laminin-1 which is typical of developing heart, suggesting that activation of regeneration is occurring in the myocardium [57].

C-Kit-positive cells have been characterized by the expression of membrane, cytoplasmic and nuclear markers, and many studies reported that cardiac precursor cells express on their surface two main antigens: stem cell factor receptor (c-Kit or CD117) and Stem cell antigen 1 (Sca-1). The expression of these markers is not univocal: one of these antigens can be expressed alone or in combination with the other [58].

1.3.1.2 Islet-1 positive cells

An interesting study performed in 2005 by Laugwitz and colleagues, revealed that mammalian heart harbors progenitor cells which are positive to Isl-1. These cells have been considered to represent the authentic, endogenous cardiac progenitor cells because they display an highly efficient conversion to a mature cardiac phenotype with stable expression of cardiac markers [59]. Since Isl-1 is a transcription factor associated with the commitment to the myocyte lineage of cardiac cells that have lost their undifferentiated stem cell fate, some authors disavowed the idea that Isl-1-positive cells are cardiac precursors; they observed that Isl-1 expression is restricted to the embryonic and fetal hearts and that Isl-1 -positive cells do not have the typical traits of stem cells [60].

However, tracing studies performed to investigate the relevance of Isl-1 -positive cells to myocardial regeneration, led to the evidence that few myocytes, SMCs and vascular ECs originated from Isl-1-positive cells [61].

1.3.1.3 Side population cells

Side population (SP) cells have been described for the first time as cells able to expel toxic compounds and dye through an ATP-binding cassette transporter, Bcrp1 [62]. These cells have been characterized for the expression of several stem markers and they resulted to be $Sca1^{high}$, c-Kit^{low}, $CD34^{low}$, and $CD45^{low}$ [63]. However, it has been observed that only the Sca1-positive CD31-negative subset of cardiac SP cells was characterized by a high cardiomyogenic potential [64].

1.3.1.4 Sca-1-positive cells

Sca-1-positive progenitor cells represent a little part of the heart, but after oxytocin treatment they express cardiac transcription factors and contractile proteins organized in sarcomeric structures [65]. Moreover, it has been shown that transplantation of sheets of Sca-1-positive cells over the necrotic area of the heart after infarction prevents negative cardiac remodeling and improves cardiac function also through the release of humoral factors which facilitate engraftment and migration of CPCs from cell sheets into host myocardium [66].

1.3.1.5 Epicardial progenitors

A pool of epicardial c-Kit-positive progenitor cells has been found in the human heart. It seems that they increase their number in hearts with chronic ischemic cardiomyopathy, and this increase is more evident in the subepicardial space than in the myocardium [57]. Moreover, these cells are able to migrate from the epicardium to the infarcted area where proliferate and differentiate into cardiomyocytes, endothelial cells and smooth muscle cells [67].

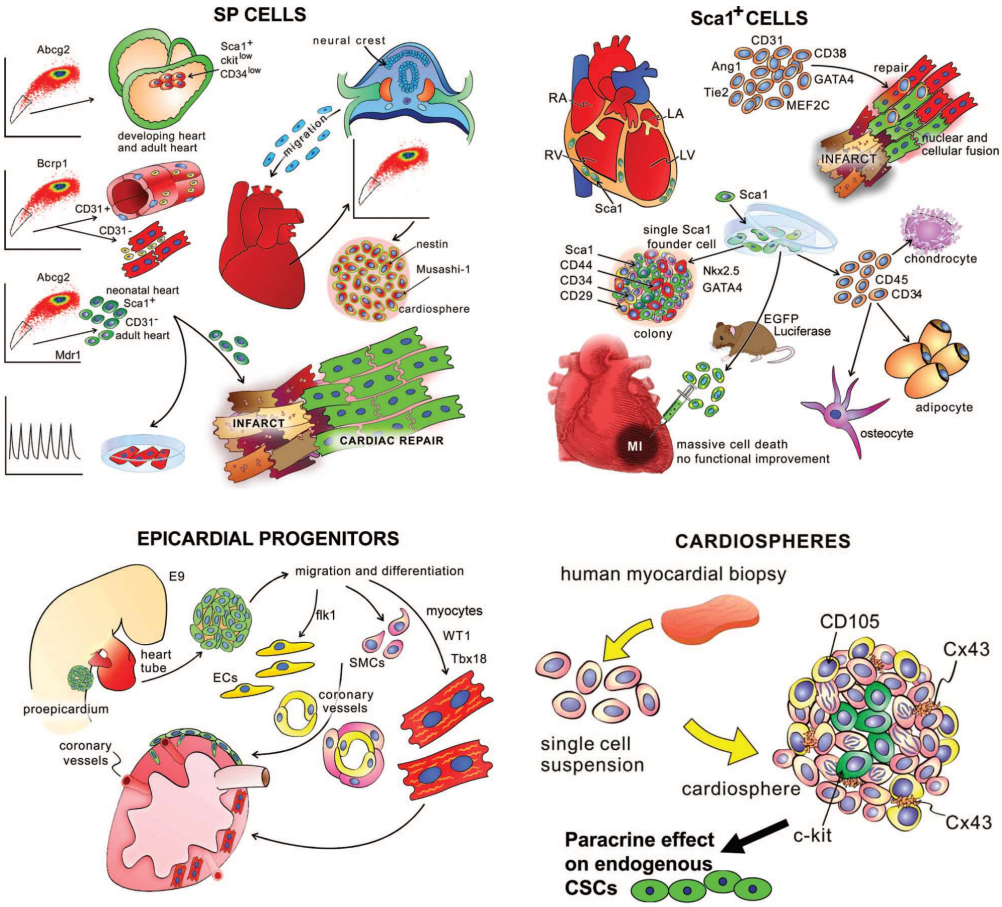

Figure 5. Cardiac progenitor cells classes. Schematic representation of population of cardiac-derived progenitor cells [54].

1.4 MiRNAs and stem cells

Increasing evidences suggest that miRNAs are also involved in regulating cell renewal and differentiation. Several studies have demonstrated that the transition from the stemness state toward the differentiated one is regulated by epigenetic mechanisms as chromatin remodeling and changes in DNA and histone modifications [68]. Since microRNAs are considered epigenetic modulators of mRNA degradation and protein translation, the idea that they can regulate stem cell maintenance and induce cell fate decision is increasingly spreading [68].

Several evidences demonstrate that microRNAs tightly control ESC self-renewal and differentiation state. Experiments of Dicer or DGC8 deletion, performed in mouse and human embryonic stem cells, confirmed a role of miRNAs in differentiation: the global loss of microRNAs resulted in proliferation and differentiation defects of embryonic stem cells [69]. Other studies identified specific sets of miRs, like miR-290 family and miR-302 family, as “embryonic stem cell-cell cycle regulating” because they repress key regulators of the cell cycle to ensure a rapid G1-S transition [70]. After induction of ESC differentiation, other microRNAs have been identified as repressors of pluripotency: miR-134, miR-296 and miR-470, repress factors responsible of pluripotency as Nanog, Oct-4 and Sox2, allowing the acquisition of differentiated phenotype [71].

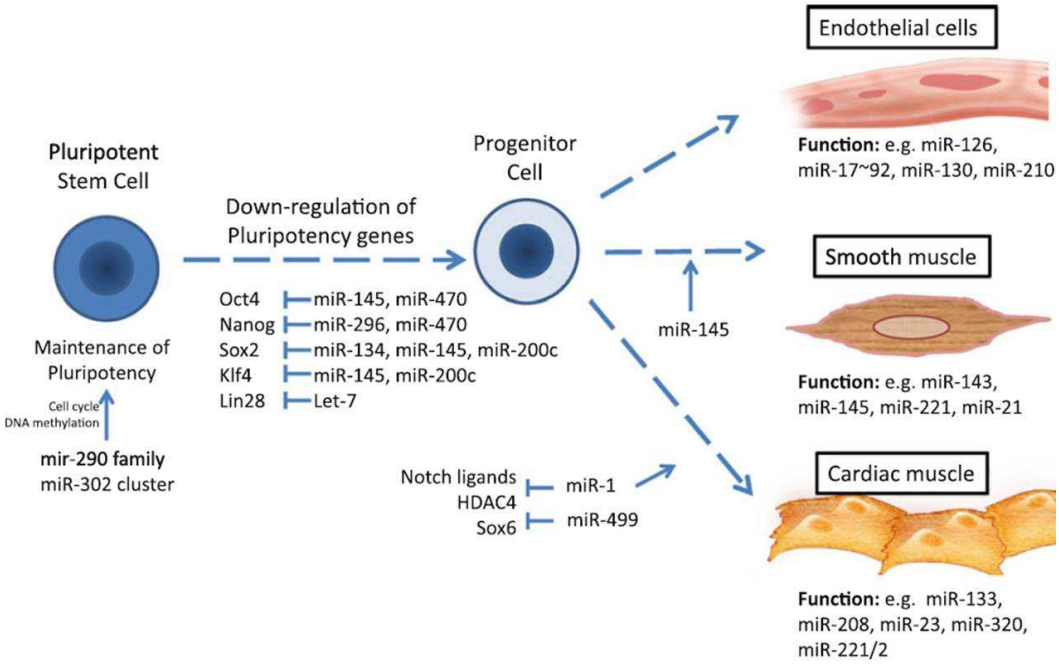

Figure 6. MicroRNAs as key factors in self-renewal and differentiation [68]

1.5 MiR-1 and miR-133: the celebrities of the heart, development and differentiation

MiR-1 and miR-133 are encoded by a duplicated locus in the mammalian genome. They are expressed by a cluster called miR-1-1/miR-133a-2 on the chromosome 2, and by a cluster called miR-1-2/miR-133a-1 on the chromosome 18. However, miR-1-1 and miR-1-2, and miR-133a-1 and miR-133a-2, originated from different loci, have the same sequence [72]. Mi-206/miR-133b cluster is transcribed from a non-coding region on the chromosome 1. MiR-206 is skeletal muscle-specific and it shares with miR-1 the same seed sequence, but they differ for 4 nucleotides in the 3'-end. Mir-133b has the same seed sequence of miR-133a-1 and miR-133a-2, and it differs just for one nucleotide in 3'end [72].

MiR-1 is highly conserved among species: comparison of genomic sequences across species revealed that a 4.6 kilobase (kb) and 10.7 kb genomic region around miR-1-1 and miR-1-2, respectively, was conserved between human and mouse. Deletion analysis have shown that the minimum region for the transcription of miR-1-1 is 2.6 kb long, and that for the transcription of miR-1-2 is just 0.35 kb long. Within these regions there are several cis elements conserved between human and mouse that represented potential binding sites for the essential cardiac transcription factors Mef2, SRF, Nkx2.5 and Gata4 [73]. Mutation of the miR-1-1 SRF site abolished miR-1 expression in the heart. This finding confirmed that the presence of miR-1 is tightly dependent on SRF [73]. Since miR-133 is located on the same locus of miR-1, it is also under the SRF control; moreover, miR-133 inhibits the expression of SRF through a negative regulating loop [74], [75].

Several studies have been performed to understand the miRNA role during cardiac development. It has been demonstrated that the miR-133a-1/miR-1-2 and miR-133a-2/miR-1-1 genes are expressed throughout the ventricular myocardium and interventricular septum from E8.5 until adulthood [73], [76].

Deletion experiments have highlighted on the importance of miRNAs in cardiac maturation. For example, in mouse, deletion of the gene coding for miR-1-2 or for miR-133 leads to alterations during cardiogenesis like the failure of ventricular

septation that results in death within few hours after birth [45], [77]. Both miR-1-1 and miR-1-2 are more expressed in the outflow tract of the heart which derives from the secondary heart field. It has also been seen that miR-1 is fundamental for cardiomyocytes differentiation, thus it has anti-proliferation effects, in fact miR-1 overexpression causes the loss of cardiomyocytes and cardiac hypoplasia which is lethal at E13.5. This event is due to the miR-1-mediated repression of Hand2, an important transcription factor involved in cardiomyocytes proliferation [73]. Experiments of deletion have shown that ≈ 50% of null mice for one of two loci of miR-1 dies from ventricular-septal defects (VSDs) between late embryogenesis and birth, while a subset of mutant mice can survive to adulthood showing electrophysiological defects. On the other hand, complete ablation of miR-133 via double gene knockout induces cardiac defects during embryogenesis, and death one day after birth (P1 stage) showing dilated atria, and enlarged, engorged with blood, and containing thrombi hearts [77]. This suggests the occurrence of defect in cardiac contractility.

A study carried in 2009 showed that small amounts of mature miR-1 and miR-133 were present in mouse undifferentiated embryonic stem cells and that expression levels of these miRNAs increased after the induction of differentiation [78].

MiR-1 and miR-133 have been identified as the most important regulators of muscle proliferation and differentiation [74]. *In vitro* studies have demonstrated that expression levels of miR-1 increase after the induction of cardiac differentiation in mouse and human embryonic stem cell-derived cardiomyocytes; moreover, the increased expression levels of miR-499 have been observed [79], [80]. Sluijter and colleagues have demonstrated that overexpression of miR-1 or miR-499 promotes early occurrence of spontaneous beating areas after differentiation of cardiomyocyte progenitor cells (CMPCs); furthermore, they have shown that miR-1 overexpression in CMPCs results in a reduction in proliferative rate and that the overexpression of miR-499 leads to an increase in the expression of cardiac transcription factors responsible of cardiac differentiation; on the other hand, the inhibition of miR-499 inhibits cardiac differentiation [79]. Although miR-1 and miR-133 are localized on the same chromosomal locus, they have different biological roles. A study performed in

2009 revealed that miR-133 represses the expression of cardiac markers in the mouse and embryonic stem cells, inducing proliferation [78]. The promotion of myocytes proliferation miR-133-mediated has been proposed to occur by repressing serum response factor (SRF) [75]; in contrast, in a more recent paper the authors found that the total ablation of miR-133 lead to an excessive cardiomyocyte proliferation, indicating that miR-133 functions as an inhibitor of cardiomyocyte proliferation; given that, the authors suggest that SRF can function as either a positive or negative regulator of cardiomyocyte proliferation and differentiation and the influence of miR-133a on downstream functions of SRF may vary depending on cofactor availability and extracellular signaling [77].

In summary, miR-1/miR-133 cluster is one of the main regulators of proliferation and differentiation of cardiac precursors. All the evidences mentioned above suggest that microRNAs play a fundamental role in regulating cell renewal and differentiation. Some authors have proposed that miRs are involved in fine control rather than in establish "on/off" decisions [68].

Since several studies suggest that overexpression of certain miRs promotes lineage commitment of stem cells, studying of these miRs could be useful for stimulation of in vitro and in vitro cell fate decision [68].

1.6 Heart regeneration

Heart is the one of the least regenerative organs in the body, thus for many years the question, which scientists have tried to answer to, was about whether there is actually no regeneration or whether it occurs at low rate. Anyway, the field of cardiac regeneration is very important to investigate because myocardial infarction in few hours can wipe out 25% of 2-4 billion cardiomyocytes that compose the human left [81]. Moreover, hypertension or valvular heart diseases kill cardiomyocytes slowly over many years and ageing causes the loss of ≈ 1 g of myocardium (that corresponds to 20 million cardiomyocytes) per year in absence of specific cardiac diseases [82], [83].

1.6.1 Heart regeneration in Zebrafish

Unlike humans, many amphibia and fish are able to regenerate limbs and internal organs after injury. Recently, it has been found that, after amputation, the apex of zebrafish heart can completely regenerate by *de novo* heart tissue rather than scar tissue [84].

To investigate which kind of cardiac cells are involved in heart regeneration, genetic fate-mapping studies have been performed. Through the creation of transgenic zebrafish, employing the drug-induced Cre/*lox* system, it has been demonstrated that heart regeneration is principally mediated by the proliferation of pre-existing cardiomyocytes, rather than by the generation of new ones from stem cells. In the same work, the authors showed that proliferating cardiomyocytes undergo limited dedifferentiantion disassembling their sarcomeric apparatus, detaching from one another and expressing regulators of cell-cycle progression [85].

1.6.2 Heart regeneration in rodents

Postnatal mammalian hearts show a lower capacity to regenerate than zebrafish hearts, but cardiomyocytes renewal during ageing and diseases occurs, even if with a lower rate.

Several studies, similar to those conducted in zebrafish model, have been performed in order to establish whether progenitor cells contribute to cardiomyocyte renewal or whether cardiac regeneration depends on proliferation of existing cardiomyocytes. Through a genetic fate-mapping study, Hsieh and colleagues have observed that the limited endogenous reparative mechanisms depended on progenitor cells-mediated regeneration rather than on replacement by cardiomyocytes proliferation [86].

Moreover, a more recent study carried out by Porrello and colleagues in 2011, has reported that, after resecting the left ventricular apex of one-day-old neonatal mice, a brisk regenerative response occured; furthermore, they have observed that this regenerative capacity was not present in seven-day-old mice and, using the

genetic fate-mapping approach, they have demonstrated that cardiac regeneration depended on pre-existing cardiomyocytes, as in zebrafish heart. The authors have proposed that the strong decrease of age-related regenerative capacity of the mouse heart is related to the reduction of cell-cycle [87].

The high regenerative capacity of adult zebrafish heart is due to its anatomical organization. In comparison with the four-chambered and double-circulation mammalian heart that works at high pressure, the fish heart is characterized by two chambers and single-circulation and thus it shows a simpler organization. The adult zebrafish heart is anatomically comparable to the embryonic mammalian heart before septation. There are also many differences in cardiomyocytes features: mammalian cardiomyocytes withdraw from the cell cycle and become bi-nucleate shortly after birth [88], while zebrafish cardiomyocytes are mononucleated and they retain proliferative potential throughout life. So, given the similarities between the adult zebrafish heart and the immature mammalian heart, some researchers have hypothesized that the mechanism that is on the base of cardiac regeneration in fish is conserved in neonatal mammalian heart [87].

1.7 Adult stem cells and biomaterials for myocardial regeneration

According to the general consent, cardiac stem cells reside in the mammalian hearts and they can probably adopt the cardiac fate. A spontaneous question that arises is: why do not cardiac stem cells work better than they do in regenerating myocardium after injury?

As it is known, cardiac cells strongly interact with the extracellular matrix (ECM) which is an essential component of the functional myocardium. ECM contains growth signals for adult myocytes, as well as mitosis, growth, differentiation and migration signals for stem and progenitor cells [89].

In the most of the studies about cardiac regeneration, the injection in the damaged heart of many types of stem cells have shown to ameliorate cardiac function but they have a low survival rate after transplantation [90]. A plausible explanation is that cardiac stem cells do not receive proper “instructions”, like signals for recruitment, activation or maturation, to accomplish cardiac regeneration. Some

reports demonstrated that after myocardium infarction, new cardiomyocytes are produced in the border region of the infarcted area but not in the middle of the damaged zone [86]. This zonal selectivity can be explained by the fact that in the border region of the infarcted area there are many capillaries that can assure the proper perfusion and, moreover, the viable myocardium and the ECM provide certain fundamental signals that are necessary to stimulate the regeneration [91].
In the last few years the strategy used by scientists to support cardiac regeneration is the employment of biomaterials to deliver these signals to transplanted stem cells. Since most stem cells are small cells, they leave within few minutes when injected in the infarcted area; for this reason biomaterials have been demonstrated to play a supporting role in maintaining of cells *in loco*.

1.7.1 Biomaterials

A biomaterial is defined as "[…] *a substance that has been engineered to take a form which, alone or as a part of a complex system, is used to direct, by control of interactions with components of living systems, the course of any therapeutic or diagnostic procedure* […]" [92]. The perfect biomaterial used in tissue regeneration should have properties of the extracellular matrix, including passive mechanical properties, signals for cell attachment, proliferation and differentiation. It should degrade without toxic metabolites production and, importantly, it should not give rise to a foreign body reaction and inflammatory response. Moreover, after implantation, biomaterials should last long enough to allow cell integration but, on the other hand, not too long to interfere with physiological coupling between differentiated cells [93].
Biomaterials used for tissue regeneration can be natural polymers, as matrigel, collagen, fibrin and synthetic polymers, as polylactic acid, polyglycolic acid and copolymers. Natural polymers can be directly extracted from animals, plants and human tissues, thus, they show good biocompatibility and low toxicity [94].
Matrigel is a protein preparation extracted from Engelbreth-Holm-Swarm mouse sarcoma. It is composed by laminin, collagen IV, heparin sulfate proteoglycan and entactin [95]. Since matrigel is extracted from living cells, it contains many

growth factors and so it could be used as an injectable hydrogel for delivery of stem cells to cardiac tissue. However, since it derives from tumor cells, it would not be appropriate for clinical applications [91].

Collagen is an ubiquitous extracellular matrix protein. It has a long, rigid triple-stranded helical structure which provides mechanical support and good environment for cell distribution and capillary formation and, moreover, its turnover is a fundamental factor in scar tissue formation and cardiac remodeling after infarct [94], [91]. Thus, collagen is very commonly used as substrate for three-dimensional *in vitro* cell culture and for *in vivo* tissue regeneration applications, because it is a nontoxic, nonimmunogenic and biodegradable compound.

Fibrin is a fibrous protein involved, with fibrinogen and thrombin, in blood clotting. It is easily available and, for this reason, is widely employed in clinical applications. Fibrin has been demonstrated to be used as an injectable biomaterial to deliver stem cells to the heart after MI [96] or for the construction of a patch for epicardial applications [97].

Although synthetic polymers are less biocompatible than the natural ones, they are used as scaffold because their degradation rate can be adapted to each specific application choosing proper polymer with proper characteristics, as porosity, three-dimensional shape and general morphology and, also because they are easily processed [94]. The most used polymers as scaffold materials are poly lactic acid (PLA) and poly glycolic acid (PGA). They are widely employed in tissue regeneration along with scaffolds to transplant cells. Because of their thermoplasticity, these polymers can be handle to form the proper shape using standard processing techniques. PGA has a simpler structure than PLA, but PLA is more hydrophobic and less crystallizable and, for this reason, it degrades slower than PGA. However, PLA dissolves easier in organic solvents [94]. Thus, they present pro and con. However, both of them are commonly used in clinical practice [98].

The challenge for cardiac regeneration after injury is to find the “perfect” biomaterial which provides the proper three-dimensional structure and the

appropriate environment for retention of stem cells after implantation in the damaged tissue and for delivery of survival and differentiation signals.

2. OBJECTIVE

The discovery of cardiac stem cells that regulate myocyte turnover has profoundly changed the knowledge of myocardial biology. This novel information imposes a reconsideration of the mechanisms involved in myocardial aging, cardiac hypertrophy and heart failure. Thus, the critical role that CSCs play in the restoration of myocardial mass and function, has been largely investigated, and the idea that cell therapy may constitute a great promise for the treatment of cardiovascular diseases has been widely spread.

Various types of adult progenitor cells have been identified and, in several studies, they showed beneficial effects in cardiac repair. For this reason they might have a therapeutic potential even if the individual subtypes of adult progenitor cells may have advantages and limitations [99].

The most important goal of regenerative medicine for the cardiac tissue is to find the best stem cell and the best way to deliver stem cells into a damage myocardium, improving their homing, integration and survival.

To achieve this purpose, the field of biomaterials has been extensively investigated because they can modulate the environment for implanted cells and enhance CSC function in the heart. Biomaterials can mimic or include naturally occurring extracellular matrix and instruct stem cell function in different ways: promoting angiogenesis, enhancing stem cell engraftment and differentiation, and accelerating electromechanical integration of transplanted cells [91].

However, stem cell function is also regulated by epigenetic factors as microRNAs. MiRNAs are small non-coding RNAs, which control gene expression by inducing mRNA degradation or by blocking mRNA translation. In the cardiovascular system miRNAs can regulate hypertrophy, apoptosis, and fibrosis [100]. Recently, it has been demonstrated that miRNAs play an important role in controlling stem cell maintenance and differentiation [68]. Thus, since several studies suggest that overexpression of certain miRs promotes lineage commitment of stem cells, the study of these miRs could be useful for stimulation of *in vivo* and *in vitro* cell fate decision [68].

According to current insights into the cardiac progenitor cells, in this project we focused our attention on the embryonic origin of these cells in the human heart,

and on the role of miRNAs during their embryonic and *in vitro* differentiation inside scaffolds.

3. MATERIAL AND METHODS

3.1 Human cardiac samples collection

Cardiac tissue samples, comprising the endocardial, myocardial, and epicardial layers of the ventricles, were obtained by autopsy from embryos, foetuses, preterm infants, and term infants and collected, after written consent from the mother, in the Department of Human Pathology of the University of Messina, Italy. Gestational age of the foetuses ranged between 9 and 40 weeks, as shown in Table 3 and Table 4. Specifically, our cohort comprised 25 samples. The causes related to the death of the analysed foetuses and of the preterm and term infants are shown in Table 3 and Table 4. Autopsies and sample collections were carried out immediately after delivery with less than a 24-hour interval since foetal death had occurred. All samples were fixed in 10% formalin and embedded in paraffin for morphological diagnostic evaluation (haematoxylin/eosin) and immunohistochemistry. Staining was performed three times per sample.

3.2 Immunohistochemistry

Single immunohistochemistry was performed by a streptavidin-biotin complex method using LSAB2 kit (DAKO Co., Carpinteria, CA, USA). After deparaffination and rehydration, the tissue sections were incubated with the protein blocking agent (DAKO) for 10 min and the primary antibody for 1 h. We used the anti-Isl-1 antibody (1:200, rabbit polyclonal, AB5754, Chemicon Int., Millipore Corp., Billerica, MA). The linked primary antibody was detected with DAKO LSAB2 streptavidin-peroxidase system according to manufacturer's instructions. 3-Amino-9-ethylcarbazole (AEC) was used as a chromogen, whereas haematoxylin was used as a light counterstain.

Double immunohistochemistry was performed by a streptavidin-biotin complex for the goat polyclonal antibody (CD105) and labelled using polymer-alkalyne phosphatase (AP) for the rabbit polyclonal antibody (c-Kit). After deparaffination and rehydration the tissue sections were incubated with the Peroxidase Block solution (Vector Laboratories Inc., Burlingame, CA) for 5 min, washed in PBS for 5 min, and incubated with the anti-CD105 goat polyclonal antibody (1:50, SC-

19793, Santa Cruz Biotechnology Inc., Santa Cruz, CA) for 30 min. After washing in PBS, sections were incubated with the biotinylated anti-goat secondary antibody (1:200, SC-2774, Santa Cruz Biotechnology Inc.) for 30 min, and washed again in PBS. For the antibody detection the streptavidin-HRP complex (LSAB2 kit DAKO) was used for 10 min. Sections were then rinsed in PBS with 0.1% Tween 20 (T-PBS) for 5 min, and incubated with 3,3'-Diaminobenzidine (DAB – Vector Laboratories) as the HRP-substrate.

After the detection of the first antigen, sections were incubated with the Doublestain Block solution (Vector Laboratories) for 3 min, washed in T-PBS for 5 min, and incubated with the anti-c-Kit rabbit polyclonal antibody (1:200, KAP-TK005, Stressgen Bioreagents, Ann Arbor, MI) for 30 min. After washing with T-PBS for 5 min, sections were incubated with a labelled polymer – AP secondary antibody (Vector Laboratories) for 30 min, and washed again. Fast red (Vector Laboratories) was used as the AP substrate for 5 min. Sections were then washed in tap water and counterstained with hematoxylin for 1 minute. DAKO Aqueous mounting medium was used. Each tissue section was analysed evaluating the percentage of positive cells in two paraffin embedded sections independently stained.

3.3 Immunofluorescence

After deparaffination and rehydration, tissue sections were blocked with 5% BSA in PBS for 30 minutes and incubated with the first primary antibody overnight, one night for each antibody (1:50, anti-c-Kit, KAP-TK005, Stressgen Bioreagents; 1:50, anti-Isl-1, goat polyclonal, SC-23590, Santa Cruz Biotechnology Inc.). After washing with PBS, cells were further incubated with fluorescent secondary antibodies 1 hour at room temperature (1:50, TRITC-conjugated anti-rabbit secondary antibody, T5268, Sigma-Aldrich, St. Louis, MO; 1:50 FITC-conjugated donkey anti-goat secondary antibody, SC-2024, Santa Cruz Biotechnology Inc.). In single immunofluorescence experiments nuclei were stained 10 minutes with 10 µg/ml Hoechst33342 staining in PBS (Invitrogen Corp., Carlsbad, CA). In confocal experiments nuclei were stained 15 minutes with 1 µM Toto-3 staining

in PBS (T3604, Invitrogen Corp.). To avoid cross-reactions, sections were incubated with goat-anti-Isl-1 first and with rabbit anti-c-Kit after, and with donkey anti-goat first and goat anti-rabbit after, in four different incubations.
To avoid autofluorescence of paraffin/formalin embedded sections, the samples were incubated in 0.1% Sudan Black in 70% ethanol for 5 minutes after nuclei staining. For imaging they were both used a Zeiss LSM5 Exciter Laser Scanning Confocal Microscope and a Leica CTR5000 fluorescent microscope. During confocal microscope observations all parameters for picture acquisition were kept the same and automatically saved.

3.4 *In situ* hybridization of human cardiac samples

In situ hybridization experiments were performed using DIG-labeled miRCURY™ detection probes (Exiqon). After section deparaffination by xylene at 56°C for 20 minutes, sections were rehydrated with decreasing ethanol scale and treated with proteinase K 10 µg/ml at 37°C for 5 minutes in order to open holes on the tissue sections to let probes recognize the complementary sequence; after treatment with 0.2% glycin in PBS for 30 seconds and washings in PBS, sections were fixed with 4% Paraformaldehyde (PFA) for 10 minutes. Afterwards, sections were pre-hybridized for 2 hours with pre-hybridization buffer [50% formamide (Sigma-Aldrich), SSC 5x, 0.1% Tween, citric acid 9.2 mM for adjustment to pH6, Heparin 50 µg/ml, yeast RNA (Applied Biosystem) 500 µg/ml] in a chamber humidified with SSC 5x and 50% formamide. Slices were incubated overnight with DIG-conjugated probes for dre-miR-133a, dre-miR-1, U6, scramble-miR (pre-designed miRCURY LNA detection probes 5'-DIG; Exiqon) (Table 1) diluted up to 20 nM in hybridization buffer, at 53°C. The day after, tissues were rinsed in SSC 2x at 53°C, 3 times in 50% formamide and SSC 2x at 53°C for 30 minutes and finally 5 times in T-PBS at room temperature. For the immunological detection of the DIG-labeled probe, slices were first treated for 1 hours at room temperature with the blocking buffer [2% sheep serum (Sigma-Aldrich Srl), 2mg/mL BSA in T-PBS] and then incubated over night at 4°C with antibody anti-DIG-AP Fab fragments (Roche Diagnostics, Germany)

diluted 1:200 in blocking buffer. After washing in T-PBS, tissues were rinsed with AP buffer (Tris HCl 100 mM, $MgCl_2$ 50 mM, NaCl 100 mM, 0.1% Tween 20, pH9.5) and then treated for the color reaction with BCIP/NBT Color Development Substrate (Promega, Madison, WI, USA) [45 µl 75vmg/ml NBT, 35µl 50vmg/ml BCIP-phosphate, 2.4 mg Levamisole (DBA Italia) in 10 ml AP buffer] for 48 hours. Tissue observation was performed with a Leica light microscope DM5000. Almost all solutions were RNase free.

Table 1. LNA enhanced oligonucleotides sequences

Probe Name	**Probe Sequence to 5'-3'**	**T(m)***
dre-miR-133°	/5DigN/CAGCTGGTTGAAGGGGACCAAA	80
dre-miR-1	/5DigN/ATACATACTTCTTTACATTCCA	63
U6, hsa/mmu/rno	/5DigN/CACGAATTTGCGTGTCATCCTT	75
Scramble	/5DigN/GTGTAACACGTCTATACGCCCA	78

*The LNA T_m was calculated using the tool accessible at www.exiqon.com

3.5 Statistical analysis

Data are shown as mean values and the standard deviation has been calculated. The hypothesis that the number of Isl-1^+ cells per mm^2 varied with the gestational age was tested using a t-test of dependent samples ($P<0.05$). The hypothesis that there was a linear correlation between the gestational age of the foetuses and the number of Isl-1^+ cells per mm^2 was tested using the Pearson coefficient ($P<0.05$). For the statistical analysis it was used the STATISTICA 6.0 software (StatSoft Italia srl, Italy).

In order to have a kinetic profile of miRNA expression in human hearts at different gestational ages, the signal was quantified. Images were first processed by adobe Photoshop CS5 in order to abolish the noise and then analyzed by

ImageJ Free software (NIH, Bethesda, MD) (http://rsb.info.nih.gov/ij/). Statistical analysis was performed using the T-test for dependent variables ($P<0.05$).

3.6 Progenitor Cells Isolation and purification

Adult Sprague–Dawley rats (up to 8 months-old), ≈ 300 g in weight, were anesthetized with: isofluoran vaporized, zoletin 20 0.20 mg/kg IM, medetomidine 0.25 mg/kg IM, atropine 0.0025 mg/kg SC. Hearts were excised still beating and put in Hank's Balanced Salt Solution (HBSS) (Sigma-Aldrich) with collagenase type II 200 U/ml (Gibco; Invitrogen Corp., Carlsbad, CA), calcium chloride 3 mmol/l and a double dose of pen/strep (Lonza). Hearts were then cut separating atria from ventricles; each ventricle has been cut into two small pieces which have been put in a fresh solution of HBSS and collagenase type II as described above. To allow the activation of the enzyme, pieces were incubated at 37°C in a rotating incubator. After that, most of the solution was centrifuged at 500 rpm for 5 minutes, while pieces remained in the rotating incubator at 37°C. These passages were repeated 10 times. The first fraction of pellets, obtained after the first five centrifugations, was discarded. The second one, got after the second five centrifugations, was filtrated with nylon net filters (Millipore) whose diameter was 80 µm, and then collected and plated in 75 cm^2 flasks with M-199 medium (BD Biosciences, Franklyn Lakes, NJ) supplemented with 20% Fetal Bovine Serum (FBS; Biolife Italiana S.r.l., Milano, Italy), fungizone 3mg/ml, streptomycin 300mg/ml, and penicillin 300 U/ml.

This method of tissue digestion allows a rapid recovery of cells with a shorter exposure of the isolated cells to the collagenase solution.

3.7 Flow cytometryc analysis

After detaching from flasks, cells were counted and placed into FACS tubes ($2x10^5$ cells/sample). Initially, cells were washed in PBS and then fixed in cold methanol on ice for 20 minutes. After washing, cells were blocked with incubation buffer (9 PBS : 1 M-199 + 10% FBS) at room temperature for 15 minutes. Cells were incubated with primary antibodies diluted 1:200 in incubation buffer for 45 minutes at room temperature [anti-c-Kit, KAP-TK005, (Stressgen Bioreagents, Ann Arbor, MI, USA); anti-Ly-6A/E (Sca-1), clone E13-161.7ne V (Santa Cruz Biotechnology, Inc); anti-MDR1, SC-71557 (Santa Cruz Biotechnology, Inc)], rinsed twice in PBS and incubated with secondary antibodies diluted 1:200 in incubation buffer for 45 minutes at room temperature in the dark. After two washes in PBS, cells were analyzed with a FACSCalibur Flow Cytometer (BD Biosciences). The unstained sample was used to calibrate the analysis.

3.8 Immunofluorescence on CPCs

Cells cultured on poly-D-lysin (Sigma – Aldrich) coated chamber slides were fixed firstly with 4% PFA for 15 min and after with ice-cold methanol for 30 min. Antigen retrieval with 10 mM citrate buffer (pH 6.0) with 0.05% Tween 20 for 10 min. After incubation with 5% Bovine Serum Albumin (Sigma – Aldrich) for 30 min, cells were incubated with primary antibodies, diluted 1:50 in PBS, overnight at 4°C [anti-c-Kit, KAP-TK005, (Stressgen Bioreagents, Ann Arbor, MI, USA); anti-Ly-6A/E (Sca-1), clone E13-161.7ne V (Santa Cruz Biotechnology, Inc); anti-MDR1, SC-71557 (Santa Cruz Biotechnology, Inc)]. Primary antibody was detected with: 1:50, FITC-conjugated anti-goat secondary antibody (Sigma – Aldrich). Nuclei were stained 10 minutes with 10 μg/ml Hoechst33342 staining in PBS (Invitrogen Corp., Carlsbad, CA). Cells were observed using Leica CTR5000 fluorescent microscope.

3.9 Tumorigenicity tests: *in vitro* and *in vivo*

3.9.1 *In vitro*

CPCs, the cell line VERO (negative control) and the cell line Hep-2 (positive control) were cultured in vitro into three different 75cm^2 flasks (BD Biosciences). Later, each cell culture (1x10^5 cells) was inoculated in six-well plates containing the solid medium (MEM plus Agar Noble, BD Bioscience) and incubated at 37°C. They were observed at inverted microscope for 3 weeks. The number of colony forming units (CFU) were counted and compared to the control (Hep-2).

3.9.2 *In vivo*

Cardiac progenitor, VERO and Hep-2 cells were inoculated in vivo by intra-cutaneous injection. Every cell type was injected in 10 Nude mice. Animals have been observed for 21 days and any new-formation of nodules in the injection area was check. The size and weight of the neoplasia were measured to evaluate the growth after 21 days. The test was considered valid if at least 9 mice inoculated with the positive control cells (Hep-2) produced a neoplasia.

3.10 Cell seeding in 2D and 3D cultures

For bi-dimensional cultures, cells were plated in 75 cm^2 flasks, grown in presence of M-199 (BD Biosciences, Franklyn Lakes, NJ, USA) grow medium, supplemented with 20% FBS (Biolife Italiana), antibiotic-antimycotic solution 1x (Lonza), L-glutamine 1x (Gibco) for 21 days, as previously described [58].
For three-dimensional cultures, cells were cultured into the Open-pore Polylactic Acid (OPLA) scaffolds (BD Biosciences) and into customized Poly(d,l) Lactic Acid [P(d,l)LA] composite scaffolds: L150609N, L150609T, L150609U (synthesized with a porosity agent less than 224 μm), L070709A (synthesized with a porosity agent less than 150 μm), kindly provided by Biotech Laboratories (University of Trento).

Before cell seeding, customized scaffolds were sterilized with 96% ethanol for 1 h. Thereafter, scaffolds were equilibrated with M-199 medium supplemented with 20% FBS, and air dried.

A mix of CSCs collagen type I rat tail (BD Biosciences) diluted 1:8 in M-199 grow medium was prepared on ice. Small pieces of scaffolds were embedded with cells and collagen mix and kept for half-hour at 37° C inside inserts for 24-well plates (BD Biosciences); each insert contained $4x10^5$cells. Then scaffolds were layered with collagen I in M-199 (dilution 1:8) and kept at 37° C for 3 hours in order to allow the solidification of collagen I. Afterwards, inserts were filled with growth medium and left in incubator for 21 days changing medium every two days.

3.10.1 P(d,l)LA scaffold microfabrication

The porous, three-dimensional P(d,l)LA scaffolds were prepared, using a solvent cast particulate leaching technique. The polymer was first dissolved in (70:30 v/v) dichloromethane/dimethylformamide solvent and then poured into a glass Petri dish containing a sufficient amount of NaCl salt. The suspension was then dried under hood overnight and washed into water for three days in order to eliminate the residual solvent and the salt. The sponges obtained were frozen at -20°C and then lyophilized for 2 days.

3.11 Transmission electron microscopy

Three-dimensional cultures were grown in M-199 medium (Life Technologies) supplemented with 20% FBS (Life Technologies) for 21 days and then fixed twice. In the first step, scaffolds were fixed with 2.5% glutaraldehyde (Electron Microscopy Sciences), in 100 mM sodium cacodylate (Life Technologies) buffer (pH 7.4) for 30 min and rinsed 3 times with 100 Mm sodium cacodylate buffer. A second step of fixation was performed with 2% OsO_4 (Electron Microscopy Sciences) in 100mM sodium cacodylate buffer. After fixation, samples were rinsed twice with 100 mM sodium cacodylate buffer (pH 7.4), and dehydrated

with ethanol (25%, 50%,70%,95% and 100%). After dehydration scaffolds were embedded into EPON resin (Electron Microscopy Sciences) with passages of 1:3 of resin/70% ethanol, 3:1 resin/70% ethanol for 2 h, pure resin overnight, pure resin with 0.1 ml DMP-30 (EMS) for 3h before inclusion and for 65°C at 48 h. Semi-thin sections were prepared and stained with Methylene Blue (Sigma - Aldrich).

3.12 RNA extraction and RT-PCR

Total RNA from cell grown for 21 days in bi-dimensional and three-dimensional cultures was purified by using ChargeSwitch® Total RNA Cell Kit (Life Technologies Europe BV Kwartsweg, Bleiswijk, Netherlands), whereas total amount of RNA from cardiac tissue was extracted using QuickPrep Total RNA Extraction Kit (GE Healthcare Bio-Sciences Corp., Piscataway, USA). RNA from both extractions was quantified by Qubit® RNA Assay Kits (Life Technologies). 5 ng total RNA per reaction was reverse-transcribed using ImProm-II Reverse Transciptase Kit (Promega Corporation, Madison, Wisconsin, USA) and GoTaq Flexi DNA Polymerase (Promega Corporation) following manufacturer's instructions. cDNA was amplified using primers listed in Table 2. Beta-actin was used as a positive control. RT-PCR products were separated on 3% agarose gel. The gel was stained with SYBR SafeDNAgel stain (Life Technologies).
ImageJ Free software (NIH, Bethesda, MD) (http://rsb.info.nih.gov/ij/) was used to obtain a numeric value for each band intensity (Mean intensity of color x Number of pixels). Values between 1 and 150,000 were considered +/-; values between 15,000 and 50,000 were considered +; values between 50,000 and 120,000 were considered ++; values between 120,000 and 200,000 were considered +++; 0 was considered – (Table 3).

Table 2. Primers used for semiquantitative reverse-transcription-polymerase chain reaction

Primers	Nucleotide sequence
Beta Actin	Fw 5**'-** AGCCATGTACGTAGCCATCG-3' Rv 5' - CTCTGAGCTGTGGTGGTGAA-3'
Laminin	Fw 5**'-** TGTAGTTCTGCAGCCATTCG-3' Rv 5**'**-CATAGGGCTGGAAGCAAGAG-3'
Integrin alpha V	Fw 5'-GCTGCCGTTGAGATAAGAGG-3' Rv 5'-TGCCTTGCTGAATGAACTTG-3'
Integrin alpha 6	Fw 5'-GGTGACTTCAAAGCCTGCTC-3' Rv 5'-AGC CAG ATC AAA AAC CAA GG-3'
Integrin alpha 7	Fw 5'-ACC TGT GCA CAC CGA TAT GA-3' Rv 5'-GCA GAA CCC AAA TTG TTC GT-3'
Integrin beta 1	Fw 5'-GAA CAG CAA GGG TGA AGC TC-3' Rv 5'-CAC AGT TGT CAC GGC ACT CT-3'
Fibronectin 1	Fw 5'-GAAAGGCAACCAGCAGAGTC-3' Rv 5'-CTGGAGTCAAGCCAGACACA-3'
ILK	Fw 5'-AAGGTGCTGAAGGTTCGAGA-3' Rv 5'-CAG TGT GTGT ATG AGG GTT GG-3'
FAK	Fw 5'-CGT GAA GCC TTT TCA AGG AG-3' Rv 5'-TCC ATC CTC ATC CGT TCT TC-3'
CgA	Fw 5'-GCC ACC AAT ACC CAA TCA CC-3' Rv 5'-CTT TAG GCC CAG CCT TCT CT-3'
Collagene V alpha	Fw 5'-GGG TGC TAG ATC AGG AGC AG-3' Rv 5'-ATG CCC ACT CCC TAA CAG TG-3'
Vitronectin	Fw 5'-ACC CTG ATT ATC CCC GAA AC-3' Rv 5'-CAA ACA CGG CTG ACA GAG AA-3'
eNOS	Fw 5'-TGA CCC TCA CCG ATA CAA CA-3' Rv 5'-CTG GCC TTC TGC TCA TTT TC -3'
Hsp90	Fw 5'-GATTGACATCATCCCCAACC-3' Rv 5'-CTG CTC ATC ATC GTT GTG CT-3'
Troponin T2	Fw 5'-CGT GAG GAG GAG GAG AAC AG-3' Rv 5'-CGG CCT CTA GGT TGT GGA TA-3'
Cardiac α MHC	Fw 5'-CTG CTC AAG GGT CTG TGT CA-3' Rv 5'-CGA ACA TGT GGT GGT TGA AG-3'
AKT	Fw 5'-CAG CAT CGG TTC TTC CTC AG-3' Rv 5'-AGA ACT GGG GGA AGT GTG TG-3'
Calmodulin	Fw 5'-ACT GGG TCA GAA CCC AAC AG-3' Rv 5'-CTT GAC CTG TCC GTC TCC AT-3'
Caveoli 3	Fw 5'-AGA CCA CTT TCA CCG TCT CC-3' Rv 5'-GCTGATGCACTGGATCTCAA-3'
CD73	Fw 5'-AGAGCAAACCAGCGATGACT-3' Rv 5'-CATTTCTGAGGAGGGGATCA-3'
CD14	Fw 5'-CTTGTTGCTGTTGCCTTTGA-3' Rv 5'-CGTGTCCACACGCTTTAGAA-3'
CD90	Fw 5'-CGAACTTCACCACCAAGGAT-3' Rv 5'-AAGGAGAGGGAAAGCAGGAG-3'
CD19	Fw 5'-TAGGCAGTGGTGCTGTGTCC-3' Rv 5'-TTCATAGGCCTCCCCTTCTT-3'

3.13 RNA extraction and Q-RT-PCR for microRNA analysis

Total RNA from cell grown for 21 days in bi-dimensional and three-dimensional cultures was purified using miRCURY™ Isolation kit (Exiqon) according to manufacturer's instructions. From each sample ≈ 90-150 ng/µl of RNA were collected.

3.14 MicroRNA qRT-PCR service and data analysis

Two samples of RNA, extracted using miRCURY™ Isolation kit (Exiqon) from CSCs grown for 21 days in 2D and 3D cultures (CSCs in a 3D collagen I matrix), were shipped on dry ice to Exiqon, Inc., which provided the service for RNA quality verification and microRNA qPCR as well as comprehensive analysis.
After RNA quality control, 40 ng of RNA was reverse transcribed into cDNA using miRCURY LNA™ Universal RT microRNA PCR, Polyadenilation and cDNA synthesis kit (Exiqon). cDNA was diluted 50x and assayed in 10 µl PCR reactions and transferred to qPCR Rodent Panel I, preloaded with 384 primers. Rno-miR-423, rno-miR-103, rno-miR-191, U6 and RNU5G were used as reference genes. Negative controls excluding template from the reverse transcription reaction was performed and profiled like the samples. The amplification was performed in a LightCycler® 480 Real-Time PCR System (Roche). The amplification curves were analyzed using the Roche LC software, both for determination of Cp (by the 2nd derivative method) and for melting curve analysis.
The amplification efficiency was calculated using algorithms similar to the LinReg software. All assays were inspected for distinct melting curves and the T_m was checked to be within known specifications for the assay. Furthermore, assays was detected with 5 Cp's less than the negative control, and with Cp<37 was included in the data analysis. Data that did not pass these criteria were omitted from any further analysis.

4. Results

4.1 Localization of cardiac stem cells and study of the expression of miRNAs in human embryos and fetuses

4.1.1 Expression of c-Kit on the membrane of cardiomyocytes of fetal hearts

In order to investigate the localization of c-Kit-positive CPCs in human embryonic and fetal hearts, immunohistochemistry and immunofluorescence experiments were performed. As shown in Figure 7A-C and summarized in Table 3, in samples from the 9^{th} to the 17^{th} gestational week, many interstitial and subepicardial cells and almost all cardiomyocytes expressed c-Kit receptor on their membrane. Even if more rarely, some c-Kit^{+} cells were found in samples at 22^{nd} gestational week. The presence of c-Kit receptor on the surface membrane of cardiomyocytes of the first and second gestational trimesters was confirmed by immunofluorescence experiments (Figure 8A, F). Panels B and C of the Figure 8 show that in the only embryonic sample, at 9^{th} week, there are some structures, similar to the primordial myocardium of the cardiac tube that are clearly positive to c-Kit. Moreover, as shown in Figure 8D, clusters of c-Kit^{+} cells are present also in samples at 15^{th} week of gestation.

4.1.2 Immunolocalization of cardiac progenitor cells

Different studies reported in literature have identified several cardiac progenitor cell populations; two of them have been described as double positive for c-Kit and CD105, in adult hearts [56] and as Isl-1-positive cell, in developing mammalian heart [59]. In order to localize separately the two populations in the human fetal heart, a double immunostaining for c-Kit and CD105, and a single immunostaining for Isl-1were performed. Results were summarized in Table 3 for c-Kit/CD105 and Table 4 for Isl-1. As shown in the panels E-F of Figure 7, interstitial c-Kit^{+}/$CD105^{+}$ cells appeared from the 17^{th} gestational week and persisted after birth, with no differences between normal hearts and fetus with heart malformation (Table 3). Double positive cells were localized in the myocardium where many dividing cells were found (Figure 7F). Single positive

cells to c-Kit were identified in the subepicardial space (Figure 7A) and in the myocardium (Figure 7C), while cells positive to CD105 were found in endocardium and endothelium as shown in Figure 1B; both of them compared from the 9^{th} to the 16^{th} gestational week.

Right and left ventricles did not show any differences in the expression of Isl-1 marker. As shown in Figure 7D and G, Isl-1^{+} cells were found in the myocardium and in the subendocardic space. Groups of Isl-1^{+} cells were sometimes visible, with a number ranging between $4.523 \pm 1.22 \times 10^{4}$ at the 14^{th} gestational week and $0.548 \pm 0.12 \times 10^{4}$ per mm^{2} in the post-natal age (Table 4, Figure 7 D,G). Statistical analysis, performed using the T-test for dependent variables, revealed that the decreasing number of Isl-1^{+} cells was significant and it depended on the gestational week. On the other hand, the number of Isl-1^{+} cells increased from the 14^{th} to the $16\text{-}19^{th}$ gestational week and it remained constant between the 20^{th} gestational week and the post-natal age. The Pearson coefficient ($r=0.5$; $P=0.14$) demonstrated that there was not a linear correlation between the gestational week and the number of cells per mm^{2}.

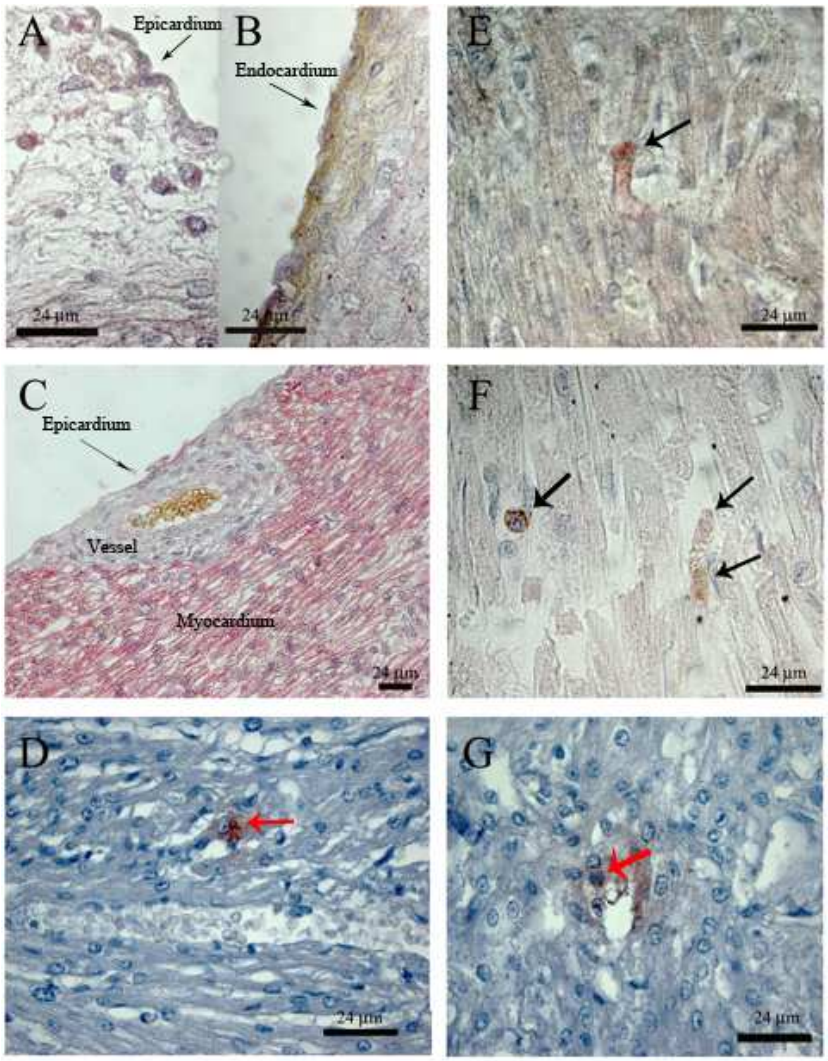

Figure 7. **Identification of interstitial c-Kit^{+}/CD105^{+} and Isl-1^{+} cells in human fetal and infant hearts before (A-D) and after (E-G) the 17th gestational week**. Immunostaining for c-Kit (Fast Red) (A-C) and CD105 (DAB) (B) in a 16-week fetal heart. E, F) c-Kit and CD105 double immunostaining in a preterm infant (36 weeks of gestation), E) and in a term infant (6-year-old child). F) Black arrows indicate double stained cells. D) Isl-1 (AEC) single immunostaining in a 14-week foetal heart; red arrows indicate Isl-1 positive cells. G) Isl-1 single immunostaining in a 21-week fetal heart. Double positive cells appeared deep red; red arrow indicate Isl-1 positive cells.

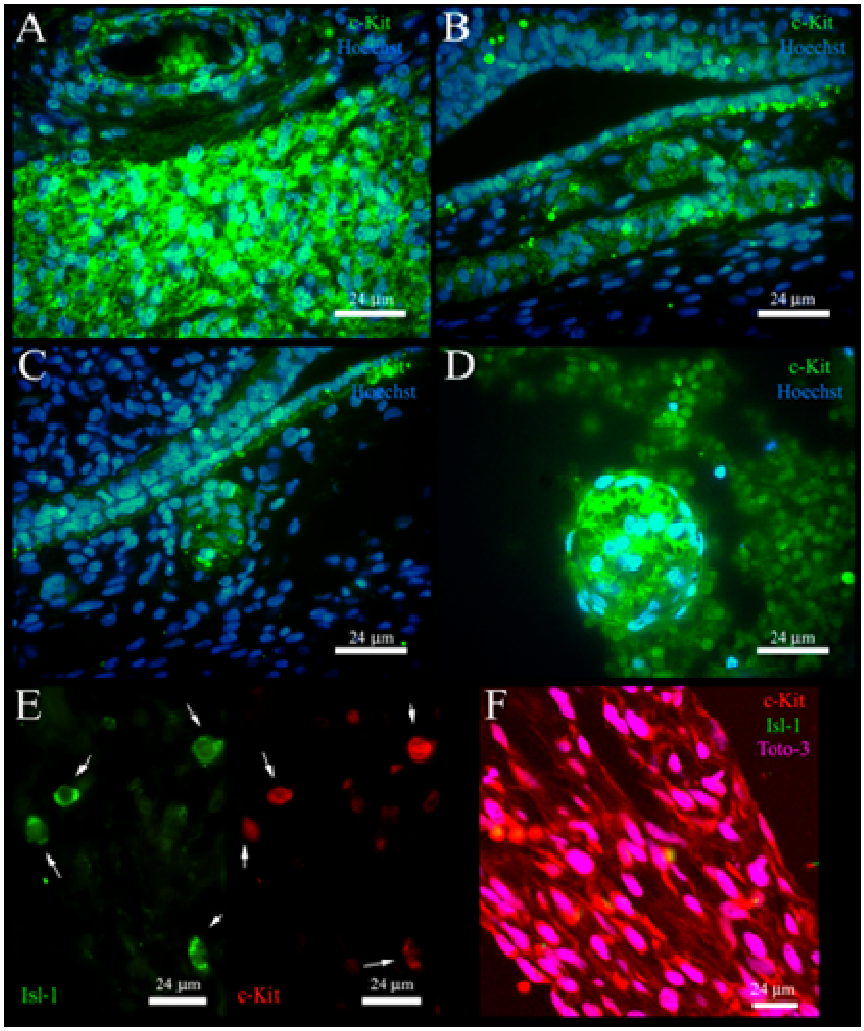

Figure 8. **Expression of c-Kit and Isl-1 in embryonic and fetal hearts.** A) Expression of c-Kit in a 16-week fetal heart. B, C) Expression of c-Kit in a 9-week human embryo. D –A cluster of c-Kit^{+} cells in a 15-week fetal heart. E) Co-localization of c-Kit^{+} and Isl-1^{+} cells in a 14-week fetal heart; white arrows indicate cells double positive for Isl-1 and c- Kit. F) Confocal microscopy analysis of the expression of c-Kit and Isl-1 in the myocardium of a 16-week fetal heart.

Table 3. Clinical and morphological data and c-Kit/CD105 expression in 1 embryo, 12 fetuses, 1 preterm infant and 1 term infant

Case No.	Trimester	Gestational age (wks)	Age at death	Cause of death	Heart malformations	Cardiomyocytes	Endocardium	Intestitial cells
Embryo								
1	I	9	9 wks	VT	Endocardial cushion defect (AVC of the heart)	c-Kit+ -	CD105+	c-Kit+/CD10
Foetuses								
2	I	13	13 wks	SA for chorioamnionitis	Absent	c-Kit+	CD105+	c-Kit+/CD105
3	II	14	14 wks	TA for CRS	VSD	c-Kit +	CD105+	c-Kit+/CD105
4	II	14	14 wks	SA for chorioamnionitis	Absent	c-Kit+	CD105+	c-Kit+/CD105
5	II	14	14 wks	TA for cerebral malformations	Absent	c-Kit+	CD105+	c-Kit+/CD105
6	II	15	15 wks	SA for chorioamnionitis	Absent	c-Kit+	CD105+	c-Kit+/CD105
7	II	16	16 wks	SA for Abruption placentae	Absent	c-Kit+	CD105+	c-Kit+/CD105
8	II	17	17 wks	TA for cerebral malformations	Absent	c-Kit+/-	CD105+	c-Kit+/CD105
9	II	18	18 wks	TA for MCA	Absent	c-Kit+/-	CD105+	c-Kit+/ CD105
10	II	19	19 wks	TA for PKD, UBH, CLGP left, PEV bilateral	Absent	c-Ki+/-	CD105+	c-Kit +/CD105
11	II	22	22 wks	SA for chorioamnionitis	Absent	c-Kit+/-	CD105+	c-Kit +/CD105
12	II	22	22 wks	SA for chorioamnionitis	Absent	c-Kit -	CD105+	c-Kit +/CD105
13	III	27	27 wks	SA for abruption placentae	Absent	c-Kit -	CD105+	c-Kit +/CD105
Preterm infant								
14	III	36	1 day	Respiratory failure	Absent	c-Kit -	CD105+	c-Kit +/CD105
Term infant								
15	III	40	6 yrs	Disseminate intravascular coagulation	Absent	c-Kit -	CD105+	c-Kit +/CD105

TA, therapeutic abortion; SA, spontaneous abortion; CLGP, cheilo-gnatho-palatischisis; CRS, caudal regression syndrome; MCA, multiple congenital anomalies; PEV, pes equino varus; PDK, polycystic kidney disease.

Table 4. Clinical and morphological data and number of Isl-1 positive cells per area (mm^2) in 7 fetuses, 2 preterm infants and 1 term infant.

Case No.	Trimester	Gestational age (wks)	Age at death	Cause of death	Growth defects	Heart malformations	Section area (mm^2)	Isl-1+ cells/mm^2 x 10^4*
Foetuses								
16	II	14	14 wks	Abruptio placentae	Absent	Absent	56171.5±11561.46	4.523±1.22
17	II	15	15 wks	TA for Prune-Belly syndrome	Absent	Absent	46063±3055.72	3.543±0.15
18	II	16	16 wks	TA for trisomy 21	IUGR	Absent	83666.33±2011.76	1.394±0.17
19	II	19	19 wks	TA for trisomy 21	Absent	Absent	71642.66±4190.29	1.141±0.62
20	II	20	20 wks	TA for trisomy 21	Absent	Absent	186604.66±9018	0.735±0.10
21	II	21	21 wks	TA for trisomy 21	Absent	Absent	119550.33±4100.16	0.889±0.14
22	II	22	22 wks	TA for cerebral malformations	Absent	Absent	162438±7750.21	0.738±0.02
Preterm infants								
23	III	26	8 days	Respiratory failure	IUGR	Ventricular septal hypertrophy	101629±1409.49	1.279±0.08
24	III	36	2 hrs	Sepsis	Absent	Ventricular septal hypertrophy	165575.33±2524.22	0.664±0.05
Term infants								
25	III	40	8 hrs	Respiratory failure	Absent	Absent	202609±13666.33	0.548±0.12

*Data for which a t-test for dependent samples was performed, $P<0.05$. Gestational weeks (independent variable); Isl-1+ cells/mm^2 (dependent variable); TA, therapeutic abortion; IUGR, intrauterin growth retardation; UBH, urinary bladder hypoplasia; VSD, ventricular septal defect; VT, voluntary termination; +, strongly positive; +/-, weakly positive.

4.1.3 Co-localization of c-Kit$^+$/Isl-1$^+$ cells

In order to investigate whether c-Kit and Isl-1 markers labeled different cell populations or not, their co-localization was evaluated by immunofluorescence experiments. It was found that all the interstitial subendocardial Isl-1$^+$ cells were positive also for c-Kit (Figure 8E), while not all the cells positive for c-Kit were also positive for Isl-1 (Figure 9A). Moreover, almost all the cardiomyocytes were c-Kit-positive (Figure 8F). The co-localization of the expression of c-Kit and Isl-1 on the same cell was confirmed by confocal microscopy (Figure 9B).

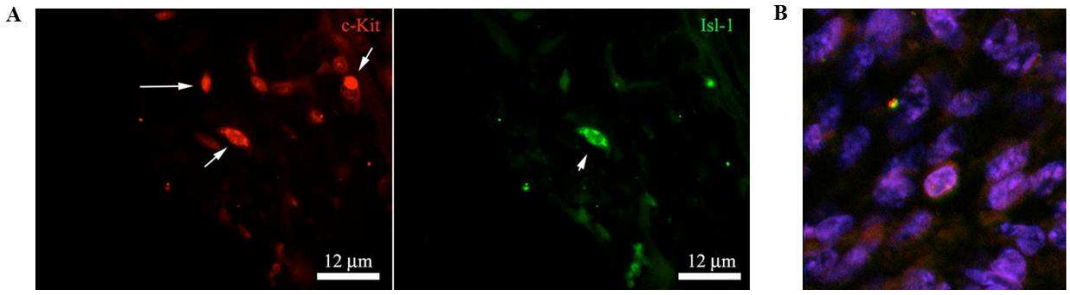

Figure 9. **Co-localization of cells positive to c-Kit and Isl-1.** A) Three cells positive to c-Kit, of which only one is also positive to Isl-1. B) Confocal microscopy enlargement of an interstitial cell positive to both c-Kit and Isl-1

4.1.4 MicroRNA expression in human heart at different gestational ages

In order to investigate how the expression levels of two of the most common expressed miRNAs in the heart, change during development, *in situ* hybridization experiments, using miR-1 and miR-133 probes, were performed. Samples from 16^{th}, 20^{th}, 32^{nd} week were analyzed. As shown in the panels A-F of figure 10, all the samples were positive for both of miRNAs with no appreciable variation among the different gestational ages, compared with controls (Figure 10G-H); nevertheless, analysis performed by the ImageJ Free software (NIH, Bethesda, MD) (http://rsb.info.nih.gov/ij/) revealed changes in miR-133 expression levels but not in miR-1 expression levels. MiR-133 significantly increased at 20^{th} gestational week and decreased at the 32^{nd} week; on the other hand, miR-1 did not undergo significant variations (Figure 10I). A light increase in miR-133 expression was observed in the bigger vessel of samples at 32^{nd} gestational week (Figure 10J-K).

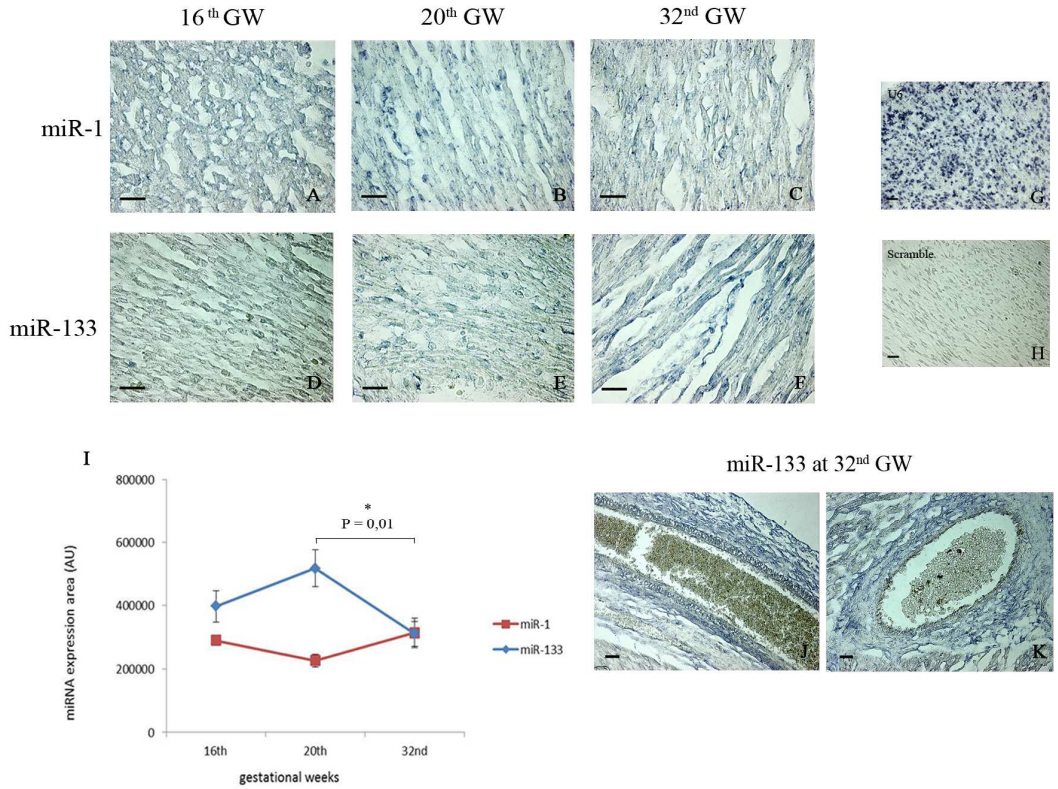

Figure 10. miR-1 and miR-133 expression in embryonic and fetal hearts by *in situ* hybridization. A-B-C) MiR-1 expression in 16-20-32-week fetal hearts; bar = 100µm D-E-F) miR-133 expression in a 16-20-32 week fetal hearts; bar = 100µm. U6 positive control (G) and Scramble negative control (H); bar = 50µm. I) Graphic representation of the variation of miR-1 and miR-133 expression levels during the three different gestational week. J-K) miR-133 expression in big vessels of 32-week fetuses; bar = 100µm (J) and 20µm (K).

4.2 Investigation on the role of miRNAs in cardiac stem cell *in vitro* differentiation

4.2.1 Cardiac stem cell isolation and characterization

Cardiac immature cells were isolated from adult rats using a differential adhesion method. Two weeks after cell isolation, a good amount of proliferating cells was obtained. Isolated cells were characterized by flow cytofluorimetric analysis and, as shown in Figure 12A, the fraction of c-Kit positive cells varied from 61.0% to 96.7% (mean 83.23 ± SD 19.3) as previously described [101], Sca-1 positive cells varied from 74.6% to 98.2% (mean 86.93% ± 11.83), MDR-1 positive cells varied from 61.1% to 72.3% (mean 63.13% ± 5.68). The expression of the three-markers was also confirmed by immunofluorescence analysis (Figure 12B-D).
In order to investigate the tumorigenic capacity of isolated cells, specific *in vivo* and *in vitro* tests were performed. 7-10 days after the beginning of the *in vitro* tumorigenicity test, Hep-2 (positive control) started to replicate producing multicellular agglomerates, while the negative cells (VERO) showed atrophy. Both the *in vitro* and *in vivo* test revealed that CPCs: There were no evidences of tumors in the several organs analyzed in mice inoculated with VERO and cardiac progenitor cells (Figure 12).

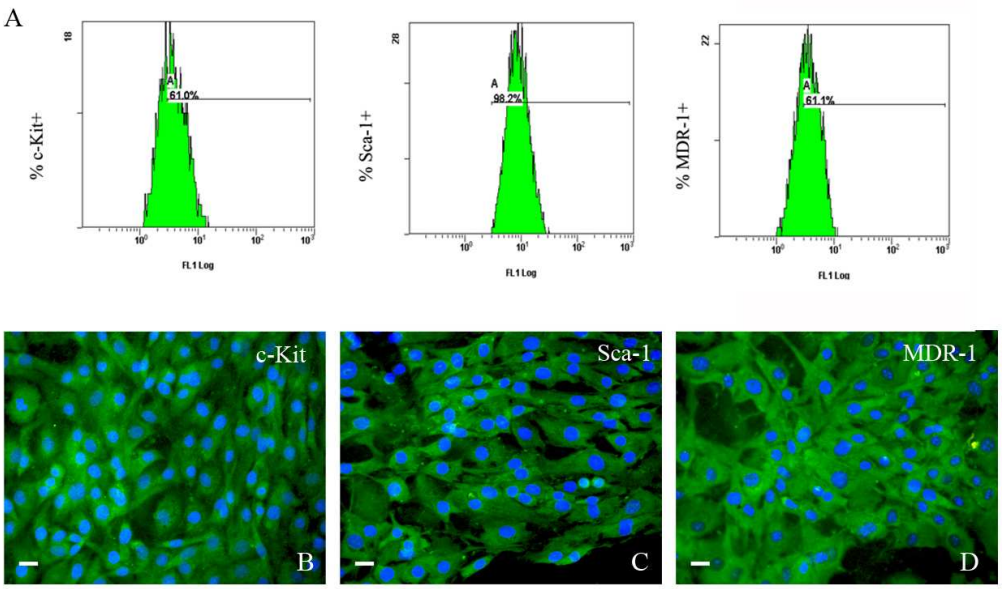

Figure 11. Cardiac progenitor cell characterization. Cytofluorimetric analysis to evaluate the percent of c-Kit, Sca-1 and MDR-1 positivity (A). Immunofluorescence analysis to c-Kit (B), Sca-1 (C) and MDR-1 (D). Bar = 20µm.

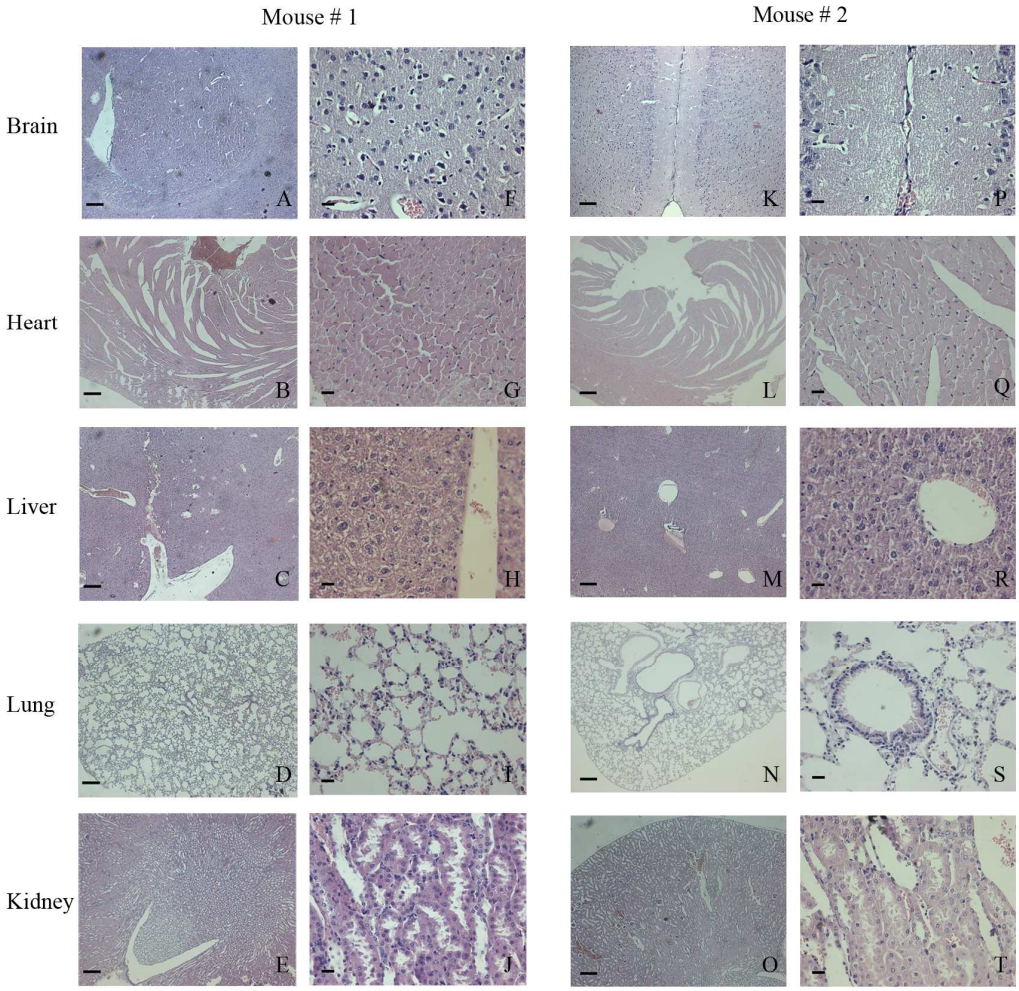

Figure 6. Histological analysis of organs after CPC inoculation in mice. Organs of two different mice were analyzed (A-J and K-T). Bar = 200µm (A-E and K-O); bar = 20 µm (F-J and P-T).

4.2.2 Cells in three-dimensional culture are partially differentiated *in vitro*: morphological evaluations

In a previous study performed in our laboratory, scaffolds were used to study the differentiation potential of CPCs [58]. In order to understand which was the better condition for cell differentiation induction, three-dimensional cultures with BD OPLA scaffolds and customized P(d,l)LA scaffolds were performed. Morphologic features of CPC grown bi-dimensional culture are shown in Figure 13A; as displayed in the panel B of the Figure 13, cells were equally distributed inside the scaffolds and perfectly embedded in the scaffold matrix.

CPCs were let grow into the scaffolds for 7, 14 and 21 days in their normal growing conditions; as shown in Figure 13C, after 21 days they expressed great amount of troponin T. Morphological analysis of semithin sections revealed that cells appeared huger and full with material similar to unorganized sarcomeric or cytoskeletal proteins (Figure 13D). A more accurate TEM observation showed the presence of caveolae on the cell membrane (Figure 13E).

Since 3D cultures were performed embedding cells in collagen I, in order to understand whether cell differentiation was depending on the presence of the three-dimensional structure offered by scaffold or not, CPCs were cultured for 21 days in 3D matrix made by collagen I, without scaffolds. Interestingly, the cytoplasm appeared more granular and better organized suggesting a higher degree of differentiation (Figure 13F).

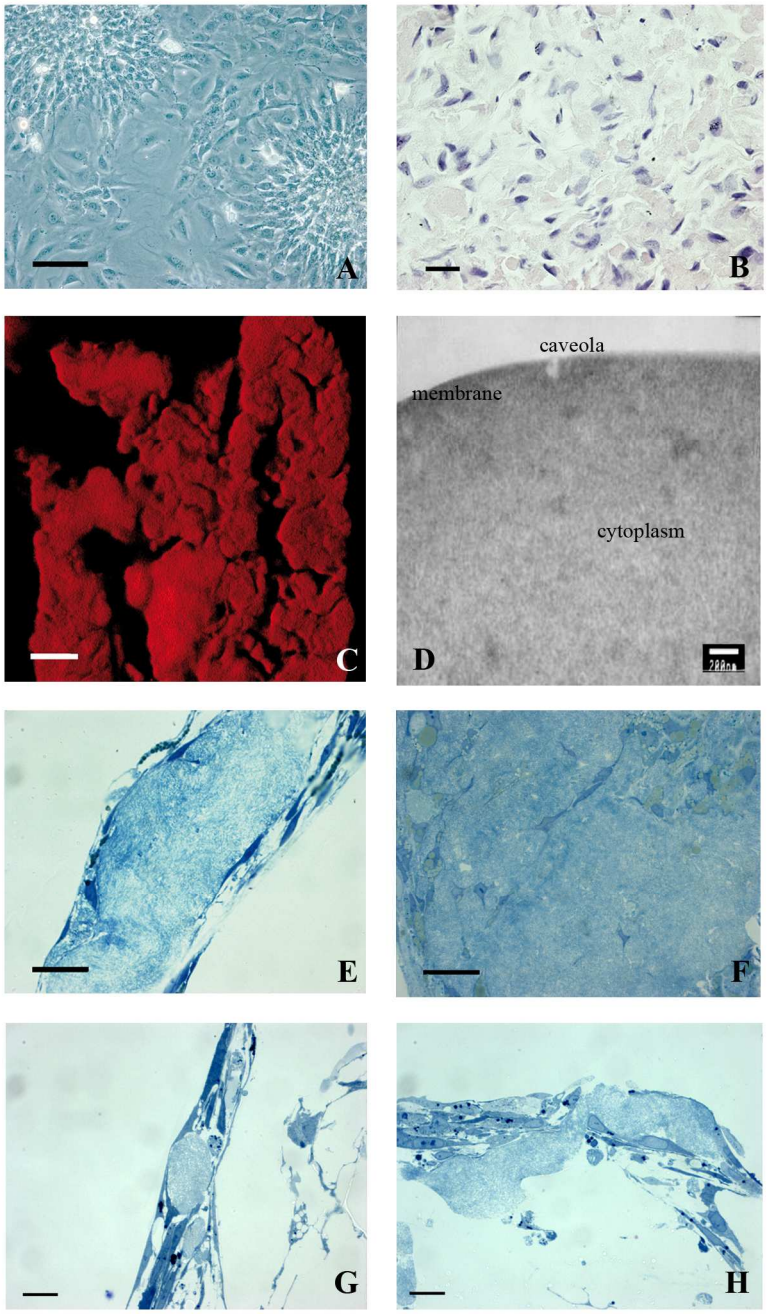

Figure 13. **CSC partially differentiate in vitro inside porous scaffolds.** Phase contrast image of isolated cells in 2D cultures (A) (bar = 100µm), ematoxilin/eosin staining of isolated cells cultured for 21 days inside BD OPLA scaffold (B), confocal scanning microscopy showing the expression of cardiac troponin T in 21 days 3D cultures inside OPLA scaffold (C), TEM image of panel E showing the cellular membrane, the cytoplasm and one caveola (D), methylene blue stained semi-thin section of 21 days 3D cultures inside BD OPLA scaffold (E). Methylene blue stained semi-thin section of 21 days 3D cultures inside collagen I (F), P(d,l)LA-N scaffold with collagen I (G), inside P(d,l)LA-U scaffold with collagen I (H). Bar = 20 µm

4.2.3 Extracellular matrix molecules expression in bi-dimensional and three-dimensional cultures

The expression of extracellular matrix proteins and their receptors is essential for the proper development and for keeping myocardium functional. For this reason, we studied the expression levels of cardiac mRNAs encoding for some extracellular matrix proteins and their receptors, some downstream signal molecules, and structural proteins in CPCs cultured in bi and three-dimensional cultures by RT-PCR.

As shown in Table 5, cells cultured for 21 days in commercial OPLA scaffolds show a low expression pattern of almost all considered genes compared with the expression pattern of cells cultured in customized P(d,l)LA scaffolds. On the other hand, although cells in three-dimensional scaffolds have been cultured in presence of collagen I, cells cultured in presence of collagen I without scaffolds show a bigger number of strongly expressed genes. Particularly, extracellular matrix proteins like laminin and fibronectin are more expressed in 3D-culture with collagen I compared to 3D-cultures with commercial and customized scaffold and 2D-cultures; the same happens in the case of almost all the ECM receptors and downstream signaling molecules as integrin classes, AKT, ILK and FAK.

Table 5. Expression of ECM molecules and receptor, cardiac-specific genes by RT-PCR

	Rat cardiac tissue	2D Culture	Collagen I only	Collagen I and BD	Collagen I and P(d,l)LA-N	Collagen I and P(d,l)LA-U
Beta-actin	+++	++	+++	+	++	++
Laminin	+	-	++	-	-	+
Fibronectin	+	++	+++	++	+++	+++
Coll V alpha	++	-	+	+	+	-
Vitronectin	++	-	-	-	+	-
Integ alpha V	+	-	+++	-	++	+
Integ alpha 6	++	-	++	+	+	+
Integ alpha 7	++	-	++	+/-	+	-
Integ beta 1	++	-	+++	+/-	++	++
ILK	++	-	+++	+	+++	++
FAK	+	-	+++	-	+	+
AKT	++	+	+++	-	++	++
Calmodulin	+++	+++	+++	+++	+++	+++
Cav3	+++	-	+++	-	+	+
CgA	++	-	-	-	+	-
eNOS	+	-	-	-	-	-
HSP90	+++	++	+++	+	++	++
Trop T2	+++	+	+++	+++	+	+
Cardiac MHC	+++	-	-	-	-	-

Note: These data were obtained analyzing the gel bands with ImageJ to obtain a numeric value for each band intensity (Mean intensity of color x Number of pixels). Values between 1 and 150,000 were considered +/-; values between 15,000 and 50,000 were considered +; values between 50,000 and 120,000 were considered ++; values between 120,000 and 200,000 were considered +++; 0 was considered -.

4.2.4 The microRNA expression in bi and three-dimensional culture of CPCs

In order to investigate the microRNA expression in CSCs grown in bi-dimensional cultures and in three-dimensional collagen matrix, the microRNA q PCR service was performed by Exiqon (Vedbaek, Denmark). The expression levels of 384 rat and mouse known microRNAs were checked. Raw data analysis reveals that the total number of expressed miRNAs was higher in cardiac stem cells grown in 3D collagen I matrix than in 2D cultures (Figure 14A); miRNA Cp average was calculated on the base of the 156 commonly expressed miRNAs; the analysis of the average highlights that miRNA expression was more induced in 3D sample rather than in 2D culture (Figure 14B).
Cp average was used to calculate the normalized Cp values which is given by:

$$\text{Normalized Cp} = \text{mean (n=156)} - \text{assay Cp}$$

Figure 14C shows the heat map diagram and the hierarchical clustering of microRNAs and samples. It is a representation of the miRNAs with the highest differential detection; for this analysis the normalized (ΔCp) values were used. Each row represents one microRNA and each column represents one sample, CSCs in 2D culture and CSCs in collagen three-dimensional matrix. The microRNA-clustering tree, shown on the left, was performed on the top 50 microRNAs with the higher standard deviation. The color scale shown at the bottom, illustrates the relative expression level of a microRNA across all samples: red color represents an expression level above the mean, green color represents expression lower than the mean. The right part of the heat map shows at the top the list of microRNAs which were more expressed in 3D cultures rather than in 2D cultures; at the bottom are listed miRNAs that were downregulated.
In order to understand how many times each miRNA was increased in 3D cultures compared to the 2D cultures, the fold change, expressed as $2^{-\Delta\Delta Cp}$, was calculated [102]. The panels D-E of the Figure 14 show the graphic representation of the most differentially expressed miRNAs comparing the two sample types. Among

50 differentially expressed miRNAs, 12 showed fold change > 1, 13 had fold change < 1.

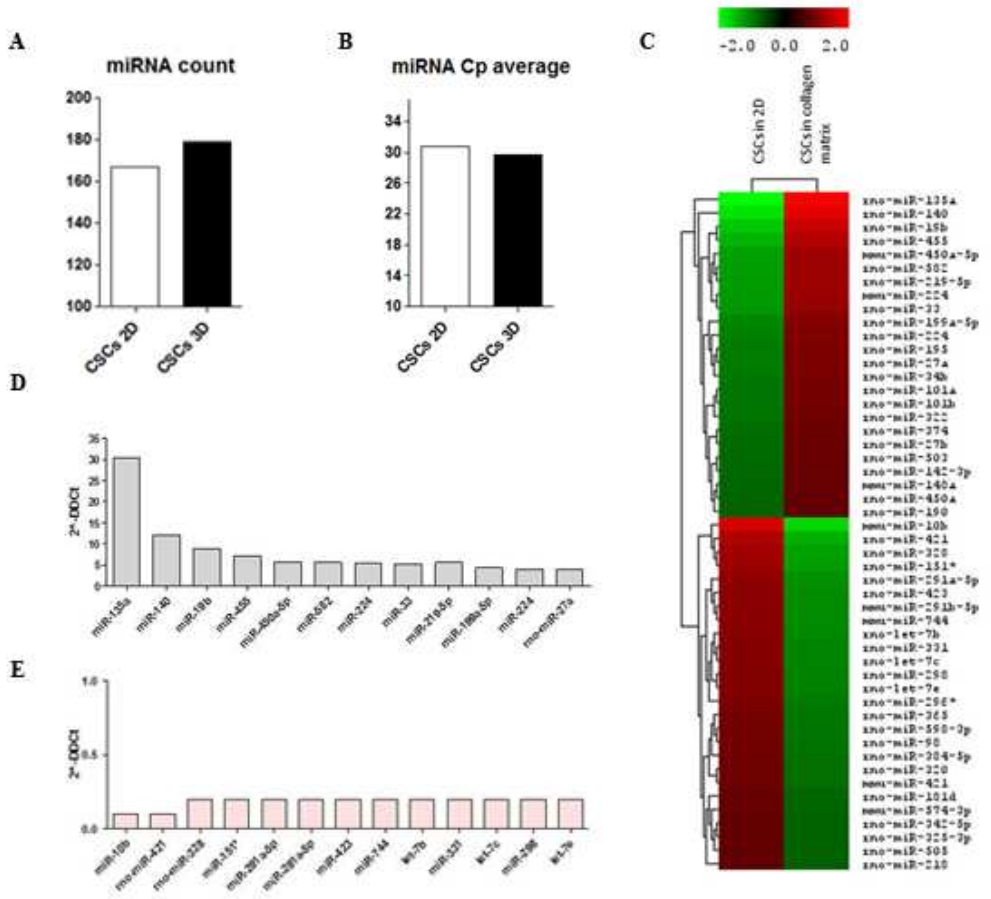

Figure 14. **microRNA expression in bi and three-dimensional culture of CPCs.** A) Total miRNA count, B) miRNA Cp average, C) heat map and hierarchical clustering, D) miRNA upregulated in CSCs grow in 3D collagen matrix E) miRNA downregulated in CSCs grow in 3D collagen matrix.

4.2.5 miR-135a and miR-140 are most differentially expressed in three-dimensional CSC culture

MicroRNA qRT-PCR service revealed that the most differentially expressed miRNAs in 3D cultures were miR-135a and miR-140 which exhibited a fold change of 30,5 and 12,1, respectively.

In order to understand if these miRNAs were conserved among species, a comparison between sequences were performed using CLC Main Workbench 5.7 software; as shown in figure 15, both considered miRNAs are perfectly conserved among rat, mouse, zebrafish and human.

The following step after the discovery of new miRNAs involved in a specific biological event is the study of their potential targets. To achieve this purpose we used one of the most widely spread engines, TargetScan (www.targetscan.org) and subsequently, DAVID bioinformatics resources (www.david.abcc.ncifcrf.gov) [103] for extracting biological meaning from large protein lists given by TargetScan.

Myocytes-enhancer factor-2 (Mef2c) is predicted to be targeted by miR-135a (Figure 16A). As can be observed, miR-135a binding site is highly conserved along the Mef2c 3'UTRs in other species (Figure 16B). Panel C of Figure 16 displays the conserved position of Mef2c 3'UTR which interacts with miR-135a seed sequence.

Target prediction analysis by TargetScan revealed that Hand2, and the regulator of differentiation 1 (Rod1), could be potential targets of miR-140 (Figure 17A and 18A). The highly conservation along the Hand2 and Rod1 3'UTRs of miR-140 binding site and the conserved position of Hand2 and Rod1 3'UTR which interacts with miR-140 seed sequence, are shown (Figure 17 B-C and 18 B-C).

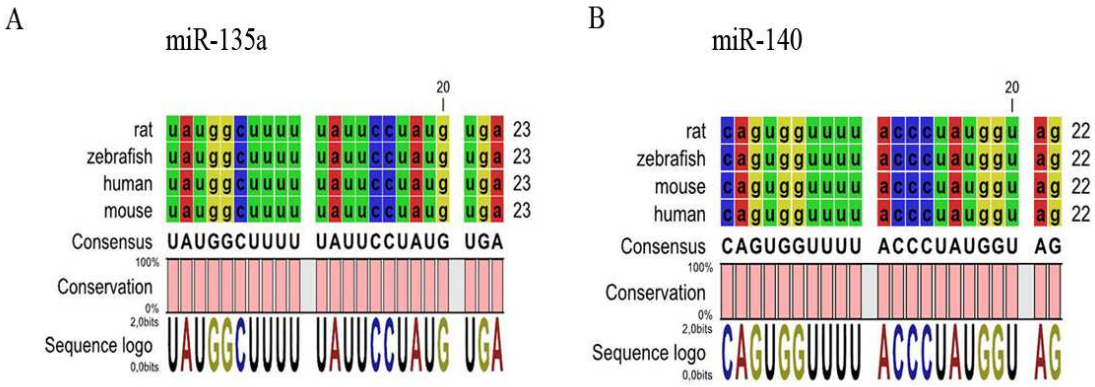

Figure 15. miRNA sequence comparison among rat, zebrafish, human and mouse. miR-135 a (A) and miR-140 (B) are conserved among species.

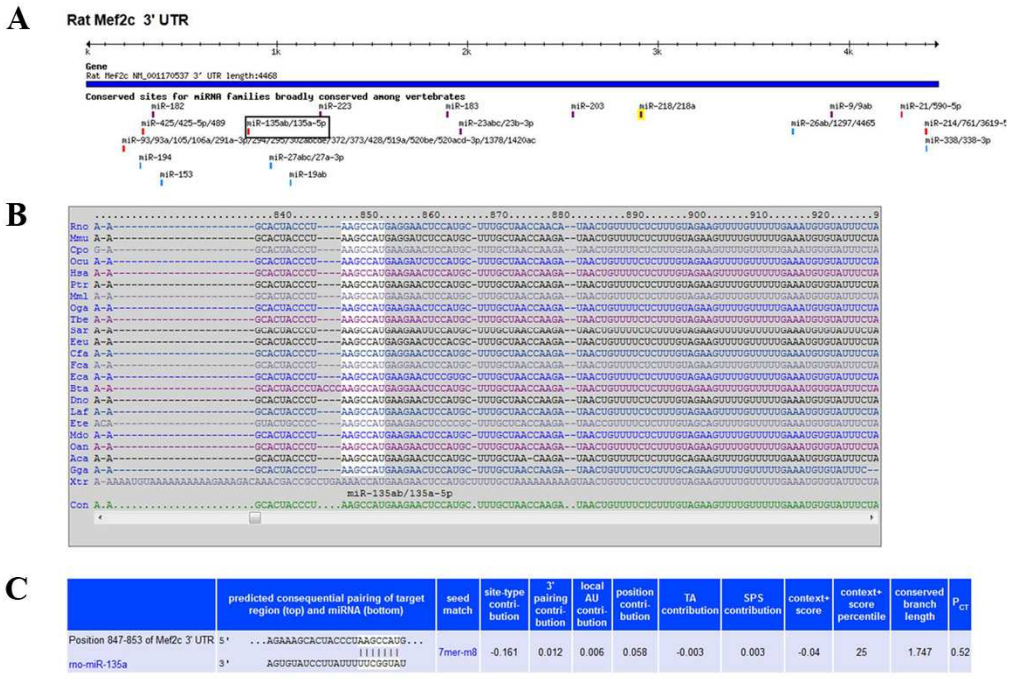

Figure 16. **TargetScan analysis of putative miR-135a binding site in the rat Mef2c transcription factor 3'UTR.** miR-135a is a putative microRNA targeting Mef2c (A) and its binding site is highly conserved along the Mef2c 3'UTR in other species (B). According to the common parameters that have to be considered, Mef2c can be considered a good potential target of miR-135a (C).

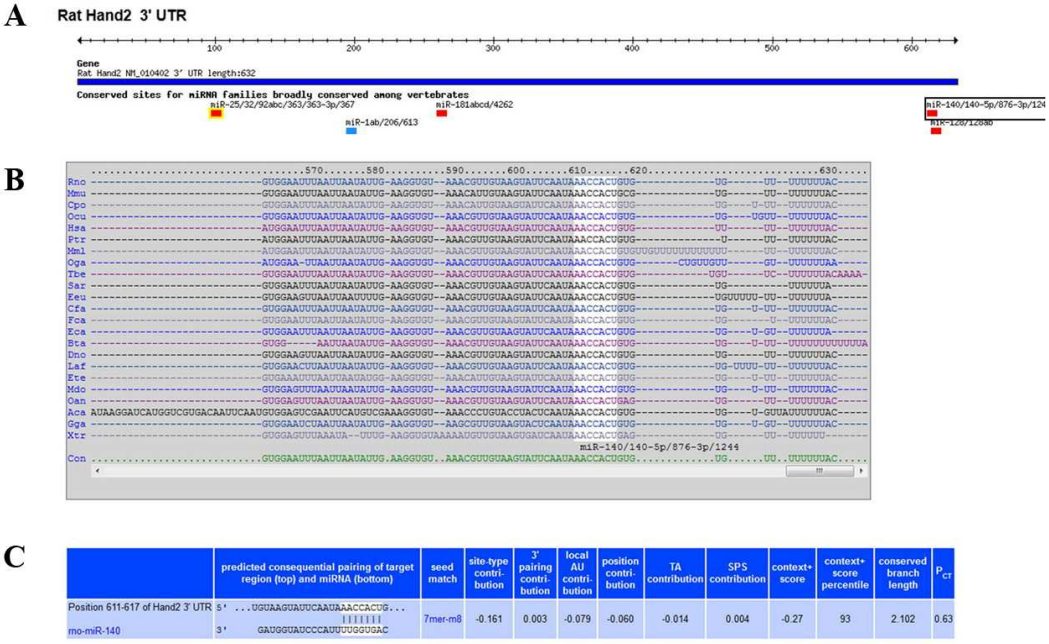

Figure 17. **TargetScan analysis of putative miR-140 binding site in the rat Hand2 3'UTR.** miR-140 is a putative microRNA targeting Hand2 (A) and its binding site is highly conserved along the Hand2 3'UTR in other species (B). According to the common parameters that have to be considered, Hand2 can be considered a good potential target of miR-140 (C).

A

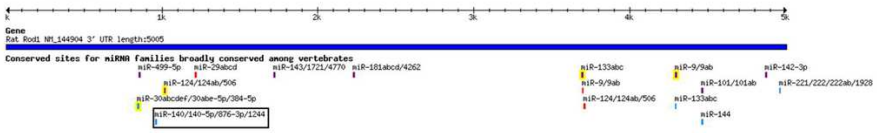

B

C

	predicted consequential pairing of target region (top) and miRNA (bottom)	seed match	site-type contribution	3' pairing contribution	local AU contribution	position contribution	TA contribution	SPS contribution	context+ score	context+ score percentile	conserved branch length	P_{CT}
Position 958-964 of Rod1 3' UTR	5' ...UCAAGGGUUUUUGUACCACUAU...	7mer-1A	-0.099	-0.006	-0.029	0.055	-0.014	-0.029	-0.10	40	1.943	0.57
mo-miR-140	3' GAUGGUAUCCCAUUU----UGGUGAC											

Figure 18. **TargetScan analysis of putative miR-140 binding site in the rat Rod1 3'UTR.** miR-140 is a putative microRNA targeting Rod1 (A) and its binding site is highly conserved along the Rod1 3'UTR in other species (B). According to the common parameters that have to be considered, Rod1 can be considered a good potential target of miR-140 (C).

5. DISCUSSION

5.1 Localization of cardiac stem cell and study of the expression of miRNAs in human embryos and fetuses

The discovery of cardiac stem cells that live in the heart and can differentiate into cardiac cell lineage, has definitely determined the shift in the ancient paradigm that heart was a terminally differentiated postmitotic organ. Several categories of cardiac stem cells have been described.

Cardiac progenitor cells can be isolated from adult and post natal hearts [104]; [59] and can be identified through the expression of several markers as c-Kit, both in fetal [67] and adult hearts [51], Isl-1 during early cardiogenesis [59]; [61] and CD105 in human endomyocardial biopsy specimens [56].

With regard to these markers, in this study we focused on the localization and temporal distribution of c-Kit$^+$/CD105$^+$ and Isl-1$^+$ cells from the embryonic to the postnatal hearts; furthermore, we tested whether c-Kit-positive cells were also present in the embryonic and fetal heart and if they represented a subset of cells different from the Isl-1$^+$ cell population.

In an attempt to define the temporal distribution and the localization of cardiac precursor cells in human hearts at different gestational ages, immunohistochemistry and immunofluorescence analysis were performed. We found that Isl-1-positive cells are present in fetuses, preterm infant and term infant human hearts. Their number decreased with the advancing of gestational age, in particular after the 16-19th week. Moreover we found that cardiomyocytes and some interstitial cells were positive to c-Kit from the 9th to the 16-19th gestational week but after this time period, the number of interstitial c-Kit-positive cells decreased. On the other hand, interstitial cells, which were double positive for c-Kit and CD105, were present only from 17th week to the 6th year of age. However, the presence of c-Kit/CD105 double positive cells in the different gestational stages does not demonstrate that c-Kit$^+$ cells are resident cardiac cells, but the fact that many structures in the embryonic heart and fetal cardiomyocytes express c-Kit provides evidence that c-Kit$^+$ cells are present in the heart from the early stages of cardiogenesis and that their number decreases with the proceeding of gestation until the postnatal age.

Moreover, Isl-1 and c-Kit co-localize in interstitial and subendocardial cells; the co-localization of the two CPC markers let us suppose that Isl-1+ cells are a subset of the c-Kit^{+} cardiac progenitor cell population. These findings are supported by a recent paper in which the authors isolated from neonate and infant specimens a pool of c-Kit positive CPCs that were also positive to Isl-1 in culture inside cardiospheres [105].

Several evidences demonstrate that microRNAs play a key role in cardiac development and cell differentiation, especially miR-1 and miR-133 are considered the main regulators in cardiogenesis [45], [77] and in cardiomyocytes differentiation [73]. In regard to literature, we wanted to investigate changing of the expression levels of miR-1 and miR-133 in human embryonic and fetal hearts during different gestational ages. In order to achieve our purpose we performed *in situ* hybridization analysis using miRCURY LNA™ DIG-labeled detection probes and we found that samples at 16th, 20th and 32nd week were positive to miR-1 and miR-133 with no appreciable variation in the different gestational weeks. In an attempt to define a kinetic profile of miR expression, the signal was quantified and, in spite of what was observed by visual analysis of the signal, miRNA expression was subject to variations: miR-133 levels significantly increased at 20th gestational week and decreases at 32nd week; on the other hand, miR-1 did not undergo to significant variations.

These findings suggest that, even if the heart is completely formed at 16th gestational week, cycles of proliferation and differentiation are still present, supporting once again that heart is not a static organ.

5.2 Investigation on miRNA expression pattern in cardiac stem cell *in vitro* differentiation

Since human heart specimens were difficult to obtain and no more information about microRNAs were recoverable, we focused our study on cardiac precursor c-Kit-positive cells isolated from adult rat heart.

According to literature, cardiac stem cells reside in the mammalian heart from the embryonic age till the adulthood, thus CSCs appear to represent ideal candidate for cardiac repair after injury. In fact, the challenge of cardiac regeneration is to find the best way to induce cardiac stem cell differentiation in the damaged heart.

The present studies on CPCs and their clinical applications regards the intramyocardial or intracoronary injection of cells. The injected cells disperse in the myocardial tissue and regenaration is very poor. A nice way to deliver CPCs in a damaged myocardium could be to use biomaterials. Moreover, the study of the expression of microRNAs in CSCs, whose overexpression can promote lineage commitment, could be useful for stimulation of *in vitro* and *in vivo* cell fate decision [68].

For all these reasons in the present study we focused on the analysis of the microRNA expression pattern in CSCs in 2D and 3D cultures, during their differentiation process.

Cardiac stem cells from adult rat myocardium were isolated and after 10 days characterized for the expression of some stem cell markers on the cell membrane. Flow cytometric analysis revealed that these cells are largely positive for all the three considered markers: c-Kit, Sca-1 and MDR-1. In order to stimulate CSC differentiation, three-dimensional cultures in PLLA scaffolds and collagen I matrix alone were performed. Morphological analysis of CPCs in 3D cultures showed a higher state of differentiation of CPCs in 3D cultures compared with 2D cultures; particularly, cytoplasm of CPCs grown in a collagen I matrix seemed to be more granular than cytoplasm of CPCs grown in P(d,l)LA or BD scaffolds. Since 3D cultures in P(d,l)LA scaffolds were prepared first embedding cells in collagen I, this evidence let us suppose that collagen I itself is responsible of differentiation.

Molecular analysis of the expression pattern of ECM coding genes, ECM receptors, downstream signaling molecules and cardiac specific genes confirmed this hypothesis. Comparison between the expression pattern of cells grown in 3D BD or P(d,l)LA scaffolds and cells in collagen I 3D-matrix revealed that genes encoding for ECM molecules, integrins, cardiac-specific proteins were more expressed in presence of collagen I only. This finding suggests once more time that collagen I is a fundamental component for cell differentiation.

For this reason we decided to investigate on the expression pattern of microRNAs in order to understand which miRNA was more induced during cardiac stem cell differentiation mediated by the presence of biomaterial.

The analysis of the genomic localization of the most differentially expressed miRNAs in three-dimensional collagen matrix cell cultures revealed that a substantial number of these miRNAs are located in intergenic regions (13/25, 52%), a big part were intronic (11/25, 44%), whereas the rest were exonic (1/25, 4%). As reported by Callis and colleagues in 2009, transcriptional regulation of gene-embedded microRNAs is modulated in accordance with transcriptional regulation of the host gene [106]. On the other hand, the transcriptional regulation of intergenic miRNAs remains largely unknown. Interestingly, in our case, several intergenic miRNAs are clustered in genomic regions and they can be transcribed as single polycistronic units and subsequently processed into single pre-miRNA molecules [107].

Surprisingly, the miRNAs whose expression we studied in embryonic and fetal hearts, miR-1 and miR-133, were not expressed. However, we found several miRNAs which were differentially expressed in CSCs grown in three-dimensional collagen I matrix rather than in CSCs grown in 2D cultures. In particular, miR-135a and miR-140 were the most differentially expressed miRNAs exhibiting the highest fold change.

MiR-135a is an intergenic miRNA whose gene is localized in the q13 of the chromosome 7 together with several quantitative trait loci (QTLs). A QTL is a chromosomal region suspected to contain a gene (or cluster of genes) that contributes to the variation observed at a quantitative trait; cardiac mass QTL6,

found in q13 of the chromosome 7, could be interesting to investigate, in order to understand whether there is a correlation with miR-135a expression.

MiR-140 is an intronic miRNA localized within the intron of NEDD4-like E3 ubiquitin-protein ligase WWP2 (intron16).

In literature there are still no evidence that these miRNAs are directly involved in cardiac stem cell differentiation, but *in silico* analysis of their predicted target revealed that both miRNAs are implicated in the regulation of two important cardiac-specific transcription factors: Mef2c (predicted target of miR-135a) and Hand2 and (predicted target of miR-140). Another potential target of miR-140 is Rod1, an RNA binding protein that negatively modulates cell differentiation [108]. In a recent paper, it has been demonstrated that Rod1 is a target of miR-499; in human CSCs, the repression of Rod1 miR-499-mediated enhanced cardiomyogenesis *in vitro* and after infarction *in vivo* [109].

Mef2c is a highly relevant transcription factor crucial for skeletal and cardiac myogenesis [110].

Hand2 is a transcription factor that promotes ventricular cardiomyocyte expansion [111]. It is a member of the basic helix loop helix (bHLH) family of transcription factors and is expressed in numerous cell lineages that contribute to the developing heart. Recently it has been demonstrated that, during cardiogenesis, Hand2, is essential for survival of second heart field progenitors and that the graded loss of Hand2 function in this cardiac progenitor pool can cause a spectrum of congenital heart malformation [112].

To study the interaction between miRNA and its target, several factors have to be assessed. Since a single miRNA can target hundreds of distinct mRNAs through seed-matched sites [113], it is important to consider that not every site is effective: 8-nt sites are effective more often than 7-nt sites, which are effective more often than 6-nt sites [29], [32]. Furthermore, another important factor is the site context. For example, sites into the 3'UTR are effective more often than those in the path of the ribosome, but among 3'UTR sites, those away from the centers of long UTR and within A-U sequence context are more often effective [29]. Other two important parameters that can influence the targeting efficacy are the weak predicted seed-pairing stability (SPS), which is a function of the concentration of

A+U in the seed region, and the high target side abundance (TA), which reflects the abundance of target sites of a miRNA family in the set of distinct 3' UTRs [114]. Thus, a negative score of SPS is associated with weaker seed-pairing stability and a negative score of TA is associated with a lower abundance of the miRNA target site in the set of 3' UTRs [114]. The sum of the contribution of all considered parameters (the site type, the local A+U content, the location of the site within the 3'UTR, SPS and TA) contributes to calculate the context+ scores for each predicted target of each miRNA. The most favorable context+ score is the lowest value [114].

According to these rules, as shown in Figure 16, 17 and 18, an accurate evaluation of the TargetScan results revealed that Mef2c, Hand2 and Rod1 seems to be good candidates for regulation mediated by miR-135a and miR-140.

In a recent work performed in 2010 by Chinchilla and colleagues, Mef2c were demonstrated to be also targeted by miR-27b, which is differentially expressed from early stages of ventricular chamber formation [115]. In the same work, the authors demonstrated that even miR-135a and miR-140 were expressed during the early stages of ventricular maturation [115].

Future investigation of the full spectrum of genes that a single miRNA may target in a given context, how these targets functionally interact, may improve our understanding of their role in the CPC biology in order to enhance cardiac stem cell ability in differentiation.

6. References

1. de la Cruz, M.V., et al., *Experimental study of the development of the truncus and the conus in the chick embryo.* J Anat, 1977. **123**(Pt 3): p. 661-86.

2. Franco, D., W.H. Lamers, and A.F. Moorman, *Patterns of expression in the developing myocardium: towards a morphologically integrated transcriptional model.* Cardiovasc Res, 1998. **38**(1): p. 25-53.

3. Bruneau, B.G., *The developmental genetics of congenital heart disease.* Nature, 2008. **451**(7181): p. 943-8.

4. Lee, R.C., R.L. Feinbaum, and V. Ambros, *The C. elegans heterochronic gene lin-4 encodes small RNAs with antisense complementarity to lin-14.* Cell, 1993. **75**(5): p. 843-54.

5. Chalfie, M., H.R. Horvitz, and J.E. Sulston, *Mutations that lead to reiterations in the cell lineages of C. elegans.* Cell, 1981. **24**(1): p. 59-69.

6. Ambros, V., *A hierarchy of regulatory genes controls a larva-to-adult developmental switch in C. elegans.* Cell, 1989. **57**(1): p. 49-57.

7. Ruvkun, G., et al., *Dominant gain-of-function mutations that lead to misregulation of the C. elegans heterochronic gene lin-14, and the evolutionary implications of dominant mutations in pattern-formation genes.* Dev Suppl, 1991. **1**: p. 47-54.

8. Reinhart, B.J., et al., *The 21-nucleotide let-7 RNA regulates developmental timing in Caenorhabditis elegans.* Nature, 2000. **403**(6772): p. 901-6.

9. Lagos-Quintana, M., et al., *Identification of novel genes coding for small expressed RNAs.* Science, 2001. **294**(5543): p. 853-8.

10. Rodriguez, A., et al., *Identification of mammalian microRNA host genes and transcription units.* Genome Res, 2004. **14**(10A): p. 1902-10.

11. Cai, X., C.H. Hagedorn, and B.R. Cullen, *Human microRNAs are processed from capped, polyadenylated transcripts that can also function as mRNAs.* RNA, 2004. **10**(12): p. 1957-66.

12. Chu, C.Y. and T.M. Rana, *Small RNAs: regulators and guardians of the genome.* J Cell Physiol, 2007. **213**(2): p. 412-9.

13. Han, J., et al., *Molecular basis for the recognition of primary microRNAs by the Drosha-DGCR8 complex.* Cell, 2006. **125**(5): p. 887-901.

14. Lund, E., et al., *Nuclear export of microRNA precursors.* Science, 2004. **303**(5654): p. 95-8.

15. Chendrimada, T.P., et al., *TRBP recruits the Dicer complex to Ago2 for microRNA processing and gene silencing.* Nature, 2005. **436**(7051): p. 740-4.

16. Lee, Y., et al., *The role of PACT in the RNA silencing pathway.* EMBO J, 2006. **25**(3): p. 522-32.

17. Hammond, S.M., et al., *An RNA-directed nuclease mediates post-transcriptional gene silencing in Drosophila cells.* Nature, 2000. **404**(6775): p. 293-6.

18. Zeng, L., et al., *Structural insights into piRNA recognition by the human PIWI-like 1 PAZ domain.* Proteins, 2011. **79**(6): p. 2004-9.

19. Liu, J., et al., *Argonaute2 is the catalytic engine of mammalian RNAi.* Science, 2004. **305**(5689): p. 1437-41.

20. Khvorova, A., A. Reynolds, and S.D. Jayasena, *Functional siRNAs and miRNAs exhibit strand bias.* Cell, 2003. **115**(2): p. 209-16.

21. Schwarz, D.S., et al., *Asymmetry in the assembly of the RNAi enzyme complex.* Cell, 2003. **115**(2): p. 199-208.

22. Okamura, K., et al., *The regulatory activity of microRNA* species has substantial influence on microRNA and 3' UTR evolution.* Nat Struct Mol Biol, 2008. **15**(4): p. 354-63.

23. Eichner, L.J., et al., *miR-378(*) mediates metabolic shift in breast cancer cells via the PGC-1beta/ERRgamma transcriptional pathway.* Cell Metab, 2010. **12**(4): p. 352-61.

24. Zhou, H., et al., *miR-155 and its star-form partner miR-155* cooperatively regulate type I interferon production by human plasmacytoid dendritic cells.* Blood, 2010. **116**(26): p. 5885-94.

25. Yang, J.S., et al., *Widespread regulatory activity of vertebrate microRNA* species.* RNA, 2011. **17**(2): p. 312-26.

26. Filipowicz, W., S.N. Bhattacharyya, and N. Sonenberg, *Mechanisms of post-transcriptional regulation by microRNAs: are the answers in sight?* Nat Rev Genet, 2008. **9**(2): p. 102-14.

27. Bartel, D.P. and C.Z. Chen, *Micromanagers of gene expression: the potentially widespread influence of metazoan microRNAs.* Nat Rev Genet, 2004. **5**(5): p. 396-400.

28. Jones-Rhoades, M.W., D.P. Bartel, and B. Bartel, *MicroRNAS and their regulatory roles in plants.* Annu Rev Plant Biol, 2006. **57**: p. 19-53.

29. Grimson, A., et al., *MicroRNA targeting specificity in mammals: determinants beyond seed pairing.* Mol Cell, 2007. **27**(1): p. 91-105.

30. Doench, J.G. and P.A. Sharp, *Specificity of microRNA target selection in translational repression.* Genes Dev, 2004. **18**(5): p. 504-11.

31. Brennecke, J., et al., *Principles of microRNA-target recognition.* PLoS Biol, 2005. **3**(3): p. e85.

32. Nielsen, C.B., et al., *Determinants of targeting by endogenous and exogenous microRNAs and siRNAs.* RNA, 2007. **13**(11): p. 1894-910.

33. Latronico, M.V., D. Catalucci, and G. Condorelli, *Emerging role of microRNAs in cardiovascular biology.* Circ Res, 2007. **101**(12): p. 1225-36.

34. Kiriakidou, M., et al., *An mRNA m7G cap binding-like motif within human Ago2 represses translation.* Cell, 2007. **129**(6): p. 1141-51.

35. Petersen, C.P., et al., *Short RNAs repress translation after initiation in mammalian cells.* Mol Cell, 2006. **21**(4): p. 533-42.

36. Parker, R. and U. Sheth, *P bodies and the control of mRNA translation and degradation.* Mol Cell, 2007. **25**(5): p. 635-46.

37. Eulalio, A., I. Behm-Ansmant, and E. Izaurralde, *P bodies: at the crossroads of post-transcriptional pathways.* Nat Rev Mol Cell Biol, 2007. **8**(1): p. 9-22.

38. Huang, J., et al., *Derepression of microRNA-mediated protein translation inhibition by apolipoprotein B mRNA-editing enzyme catalytic polypeptide-like 3G (APOBEC3G) and its family members.* J Biol Chem, 2007. **282**(46): p. 33632-40.

39. Betel, D., et al., *The microRNA.org resource: targets and expression.* Nucleic Acids Res, 2008. **36**(Database issue): p. D149-53.

40. Lewis, B.P., et al., *Prediction of mammalian microRNA targets.* Cell, 2003. **115**(7): p. 787-98.

41. Krek, A., et al., *Combinatorial microRNA target predictions.* Nat Genet, 2005. **37**(5): p. 495-500.

42. Kertesz, M., et al., *The role of site accessibility in microRNA target recognition.* Nat Genet, 2007. **39**(10): p. 1278-84.

43. Boyd, S.D., *Everything you wanted to know about small RNA but were afraid to ask.* Lab Invest, 2008. **88**(6): p. 569-78.

44. Morton, S.U., et al., *microRNA-138 modulates cardiac patterning during embryonic development.* Proc Natl Acad Sci U S A, 2008. **105**(46): p. 17830-5.

45. Zhao, Y., et al., *Dysregulation of cardiogenesis, cardiac conduction, and cell cycle in mice lacking miRNA-1-2.* Cell, 2007. **129**(2): p. 303-17.

46. Rao, P.K., et al., *Loss of cardiac microRNA-mediated regulation leads to dilated cardiomyopathy and heart failure.* Circ Res, 2009. **105**(6): p. 585-94.

47. Ikeda, S., et al., *Altered microRNA expression in human heart disease.* Physiol Genomics, 2007. **31**(3): p. 367-73.

48. Anversa, P. and J. Kajstura, *Ventricular myocytes are not terminally differentiated in the adult mammalian heart.* Circ Res, 1998. **83**(1): p. 1-14.

49. Urbanek, K., et al., *Stem cell niches in the adult mouse heart.* Proc Natl Acad Sci U S A, 2006. **103**(24): p. 9226-31.

50. Hosoda, T., et al., *Role of stem cells in cardiovascular biology.* J Thromb Haemost, 2011. **9 Suppl 1**: p. 151-61.

51. Di Felice, V., et al., *Cardiac stem cell research: an elephant in the room?* Anat Rec (Hoboken), 2009. **292**(3): p. 449-54.

52. Anversa, P. and B. Nadal-Ginard, *Myocyte renewal and ventricular remodelling.* Nature, 2002. **415**(6868): p. 240-3.

53. Rubart, M. and L.J. Field, *Cardiac regeneration: repopulating the heart.* Annu Rev Physiol, 2006. **68**: p. 29-49.

54. Leri, A., J. Kajstura, and P. Anversa, *Role of cardiac stem cells in cardiac pathophysiology: a paradigm shift in human myocardial biology.* Circ Res, 2011. **109**(8): p. 941-61.

55. Beltrami, A.P., et al., *Adult cardiac stem cells are multipotent and support myocardial regeneration.* Cell, 2003. **114**(6): p. 763-76.

56. Smith, R.R., et al., *Regenerative potential of cardiosphere-derived cells expanded from percutaneous endomyocardial biopsy specimens.* Circulation, 2007. **115**(7): p. 896-908.

57. Castaldo, C., et al., *CD117-positive cells in adult human heart are localized in the subepicardium, and their activation is associated with laminin-1 and alpha6 integrin expression.* Stem Cells, 2008. **26**(7): p. 1723-31.

58. Di Felice, V., et al., *OPLA scaffold, collagen I, and horse serum induce an higher degree of myogenic differentiation of adult rat cardiac stem cells.* J Cell Physiol, 2009. **221**(3): p. 729-39.

59. Laugwitz, K.L., et al., *Postnatal isl1+ cardioblasts enter fully differentiated cardiomyocyte lineages.* Nature, 2005. **433**(7026): p. 647-53.

60. Leri, A., *Human cardiac stem cells: the heart of a truth.* Circulation, 2009. **120**(25): p. 2515-8.

61. Moretti, A., et al., *Multipotent embryonic isl1+ progenitor cells lead to cardiac, smooth muscle, and endothelial cell diversification.* Cell, 2006. **127**(6): p. 1151-65.

62. Hierlihy, A.M., et al., *The post-natal heart contains a myocardial stem cell population.* FEBS Lett, 2002. **530**(1-3): p. 239-43.

63. Rasmussen, T.L., et al., *Getting to the heart of myocardial stem cells and cell therapy.* Circulation, 2011. **123**(16): p. 1771-9.

64. Pfister, O., et al., *Role of the ATP-binding cassette transporter Abcg2 in the phenotype and function of cardiac side population cells.* Circ Res, 2008. **103**(8): p. 825-35.

65. Matsuura, K., et al., *Adult cardiac Sca-1-positive cells differentiate into beating cardiomyocytes.* J Biol Chem, 2004. **279**(12): p. 11384-91.

66. Matsuura, K., et al., *Transplantation of cardiac progenitor cells ameliorates cardiac dysfunction after myocardial infarction in mice.* J Clin Invest, 2009. **119**(8): p. 2204-17.

67. Limana, F., et al., *Identification of myocardial and vascular precursor cells in human and mouse epicardium.* Circ Res, 2007. **101**(12): p. 1255-65.

68. Ohtani, K. and S. Dimmeler, *Control of cardiovascular differentiation by microRNAs.* Basic Res Cardiol, 2011. **106**(1): p. 5-11.

69. Martinez, N.J. and R.I. Gregory, *MicroRNA gene regulatory pathways in the establishment and maintenance of ESC identity.* Cell Stem Cell, 2010. **7**(1): p. 31-5.

70. Wang, Y., et al., *Embryonic stem cell-specific microRNAs regulate the G1-S transition and promote rapid proliferation.* Nat Genet, 2008. **40**(12): p. 1478-83.

71. Tay, Y., et al., *MicroRNAs to Nanog, Oct4 and Sox2 coding regions modulate embryonic stem cell differentiation.* Nature, 2008. **455**(7216): p. 1124-8.

72. Townley-Tilson, W.H., T.E. Callis, and D. Wang, *MicroRNAs 1, 133, and 206: critical factors of skeletal and cardiac muscle development, function, and disease.* Int J Biochem Cell Biol, 2010. **42**(8): p. 1252-5.

73. Zhao, Y., E. Samal, and D. Srivastava, *Serum response factor regulates a muscle-specific microRNA that targets Hand2 during cardiogenesis.* Nature, 2005. **436**(7048): p. 214-20.

74. Chen, J.F., et al., *The role of microRNA-1 and microRNA-133 in skeletal muscle proliferation and differentiation.* Nat Genet, 2006. **38**(2): p. 228-33.

75. Niu, Z., et al., *Serum response factor micromanaging cardiogenesis.* Curr Opin Cell Biol, 2007. **19**(6): p. 618-27.

76. Liu, N., et al., *An intragenic MEF2-dependent enhancer directs muscle-specific expression of microRNAs 1 and 133.* Proc Natl Acad Sci U S A, 2007. **104**(52): p. 20844-9.

77. Liu, N., et al., *microRNA-133a regulates cardiomyocyte proliferation and suppresses smooth muscle gene expression in the heart.* Genes Dev, 2008. **22**(23): p. 3242-54.

78. Takaya, T., et al., *MicroRNA-1 and MicroRNA-133 in spontaneous myocardial differentiation of mouse embryonic stem cells.* Circ J, 2009. **73**(8): p. 1492-7.

79. Sluijter, J.P., et al., *MicroRNA-1 and -499 regulate differentiation and proliferation in human-derived cardiomyocyte progenitor cells.* Arterioscler Thromb Vasc Biol, 2010. **30**(4): p. 859-68.

80. Wilson, K.D., et al., *Dynamic microRNA expression programs during cardiac differentiation of human embryonic stem cells: role for miR-499.* Circ Cardiovasc Genet, 2010. **3**(5): p. 426-35.

81. Murry, C.E., H. Reinecke, and L.M. Pabon, *Regeneration gaps: observations on stem cells and cardiac repair.* J Am Coll Cardiol, 2006. **47**(9): p. 1777-85.

82. Whelan, R.S., V. Kaplinskiy, and R.N. Kitsis, *Cell death in the pathogenesis of heart disease: mechanisms and significance.* Annu Rev Physiol, 2010. **72**: p. 19-44.

83. Olivetti, G., et al., *Cardiomyopathy of the aging human heart. Myocyte loss and reactive cellular hypertrophy.* Circ Res, 1991. **68**(6): p. 1560-8.

84. Poss, K.D., L.G. Wilson, and M.T. Keating, *Heart regeneration in zebrafish.* Science, 2002. **298**(5601): p. 2188-90.

85. Jopling, C., et al., *Zebrafish heart regeneration occurs by cardiomyocyte dedifferentiation and proliferation.* Nature, 2010. **464**(7288): p. 606-9.

86. Hsieh, P.C., et al., *Evidence from a genetic fate-mapping study that stem cells refresh adult mammalian cardiomyocytes after injury.* Nat Med, 2007. **13**(8): p. 970-4.

87. Porrello, E.R., et al., *Transient regenerative potential of the neonatal mouse heart.* Science, 2011. **331**(6020): p. 1078-80.

88. Walsh, S., et al., *Cardiomyocyte cell cycle control and growth estimation in vivo--an analysis based on cardiomyocyte nuclei.* Cardiovasc Res, 2010. **86**(3): p. 365-73.

89. Lutolf, M.P. and J.A. Hubbell, *Synthetic biomaterials as instructive extracellular microenvironments for morphogenesis in tissue engineering.* Nat Biotechnol, 2005. **23**(1): p. 47-55.

90. Segers, V.F. and R.T. Lee, *Stem-cell therapy for cardiac disease.* Nature, 2008. **451**(7181): p. 937-42.

91. Segers, V.F. and R.T. Lee, *Biomaterials to enhance stem cell function in the heart.* Circ Res, 2011. **109**(8): p. 910-22.

92. Williams, D.F., *On the nature of biomaterials.* Biomaterials, 2009. **30**(30): p. 5897-909.

93. Davis, M.E., et al., *Custom design of the cardiac microenvironment with biomaterials.* Circ Res, 2005. **97**(1): p. 8-15.

94. Carletti, E., A. Motta, and C. Migliaresi, *Scaffolds for tissue engineering and 3D cell culture.* Methods Mol Biol, 2011. **695**: p. 17-39.

95. Kleinman, H.K. and G.R. Martin, *Matrigel: basement membrane matrix with biological activity.* Semin Cancer Biol, 2005. **15**(5): p. 378-86.

96. Danoviz, M.E., et al., *Rat adipose tissue-derived stem cells transplantation attenuates cardiac dysfunction post infarction and biopolymers enhance cell retention.* PLoS One, 2010. **5**(8): p. e12077.

97. Liu, J., et al., *Autologous stem cell transplantation for myocardial repair.* Am J Physiol Heart Circ Physiol, 2004. **287**(2): p. H501-11.

98. Athanasiou, K.A., G.G. Niederauer, and C.M. Agrawal, *Sterilization, toxicity, biocompatibility and clinical applications of polylactic acid/polyglycolic acid copolymers.* Biomaterials, 1996. **17**(2): p. 93-102.

99. Dimmeler, S. and D. Losordo, *Stem cells review series: an introduction.* Circ Res, 2011. **109**(8): p. 907-9.

100. Small, E.M., R.J. Frost, and E.N. Olson, *MicroRNAs add a new dimension to cardiovascular disease.* Circulation, 2010. **121**(8): p. 1022-32.

101. Bolli, R., et al., *Cardiac stem cells in patients with ischaemic cardiomyopathy (SCIPIO): initial results of a randomised phase 1 trial.* Lancet, 2011. **378**(9806): p. 1847-57.

102. Livak, K.J. and T.D. Schmittgen, *Analysis of relative gene expression data using real-time quantitative PCR and the 2(-Delta Delta C(T)) Method.* Methods, 2001. **25**(4): p. 402-8.

103. Huang da, W., B.T. Sherman, and R.A. Lempicki, *Systematic and integrative analysis of large gene lists using DAVID bioinformatics resources.* Nat Protoc, 2009. **4**(1): p. 44-57.

104. Anversa, P., et al., *Concise review: stem cells, myocardial regeneration, and methodological artifacts.* Stem Cells, 2007. **25**(3): p. 589-601.

105. Mishra, R., et al., *Characterization and functionality of cardiac progenitor cells in congenital heart patients.* Circulation, 2011. **123**(4): p. 364-73.

106. Callis, T.E., et al., *MicroRNA-208a is a regulator of cardiac hypertrophy and conduction in mice.* J Clin Invest, 2009. **119**(9): p. 2772-86.

107. Fazi, F. and C. Nervi, *MicroRNA: basic mechanisms and transcriptional regulatory networks for cell fate determination.* Cardiovasc Res, 2008. **79**(4): p. 553-61.

108. Yamamoto, H., et al., *Isolation of a mammalian homologue of a fission yeast differentiation regulator.* Mol Cell Biol, 1999. **19**(5): p. 3829-41.

109. Hosoda, T., et al., *Human cardiac stem cell differentiation is regulated by a mircrine mechanism.* Circulation, 2011. **123**(12): p. 1287-96.

110. Edmondson, D.G., et al., *Mef2 gene expression marks the cardiac and skeletal muscle lineages during mouse embryogenesis.* Development, 1994. **120**(5): p. 1251-63.

111. Yelon, D., et al., *The bHLH transcription factor hand2 plays parallel roles in zebrafish heart and pectoral fin development.* Development, 2000. **127**(12): p. 2573-82.

112. Tsuchihashi, T., et al., *Hand2 function in second heart field progenitors is essential for cardiogenesis.* Dev Biol, 2011. **351**(1): p. 62-9.

113. Lim, L.P., et al., *Microarray analysis shows that some microRNAs downregulate large numbers of target mRNAs.* Nature, 2005. **433**(7027): p. 769-73.

114. Garcia, D.M., et al., *Weak seed-pairing stability and high target-site abundance decrease the proficiency of lsy-6 and other microRNAs.* Nat Struct Mol Biol, 2011. **18**(10): p. 1139-46.

115. Chinchilla, A., et al., *MicroRNA profiling during mouse ventricular maturation: a role for miR-27 modulating Mef2c expression.* Cardiovasc Res, 2011. **89**(1): p. 98-108.

ACKNOWLEDGEMENTS

At the end of these three years I would like to sincerely thank first of all Professor Giovanni Zummo, head of department of Experimental Biomedicine and Clinical Neurosciences. He is a high moral stature man, a guide and a good role model for my life.
Then, I want to thank Professor Francesco Cappello and all the other lecturers of the Human Anatomy section because they all have contributed to my training.
A special thanks goes to my co-tutor, Dr. Valentina Di Felice, because she accompanied me during this period and she was an example of ambition and perseverance.

I spent the last seven months of my PhD course at Université Pierre et Marie Curie of Paris working with the equipe of Génétique et Physiopathologie des Tessus Musculaires (UR4 – Vieillissement, Stress et Inflammation) directed by Dr. Zhenlin Li, under the supervision of Dr. Dario Coletti.
I am very grateful to Dr. Coletti, who was a fundamental model helping me in my daily life and in scientific questions too. It was exciting and very stimulating to work with him and with his equipe. They taught me how to approach to the microRNA prediction target analysis, offering proper software and all their expertise. Moreover, I would like to thank Dr. Coletti for having involved me in one of his project regarding to the *in vitro* study of cachexia-inducing factors on proliferation, differentiation and death of cardiac cell lineage.

Finally, at last but not least, I give thanks to all my colleagues, who aided me when I was in trouble and shared with me joys and sorrows during these three years. I want to sincerely say thanks for their true friendship. I am sure the love that binds us will continue all over the time.